Z. Zhang[1,2], F. Chen[3], M. Barlage[4], L.E. Bortolotti[1,5], J. Famiglietti[1,2], Z. Li[2], X. Ma[1,2], Y. Li[1,2]*

[1] School of Environment and Sustainablity, University of Saskatchewan, SK, Canada

[2] Global Institute for Water Security, University of Saskatchewan, SK, Canada

[3] Research Application Laboratory, National Center for Atmospheric Research, Boulder, CO, USA

[4] Environmental Modeling Center, National Oceanic and Atmospheric Administration, College Park, MD, USA

[5] Institute for Wetland and Waterfowl Research, Ducks Unlimited Canada, Stonewall, MB, Canada

Corresponding author: Dr. Yanping Li (`yanping.li@usask.ca`)

Key Points:

- An updated parameterization for wetlands reasonably captures spatial extent and seasonal variation in the Prairie Pothole Region.

- Implementing this wetland parameterization in Noah-MP LSM shows strong impacts on surface energy and water budget.

- Wetlands' effects on regional climate is strong and evident, especially in cooling summer temperatures, greatly mitigating heat stress from heatwaves.

Abstract

Wetlands are an important land type – they provide vital ecosystem services such as regulating floods, storing carbon, and providing wildlife habitat. The ability to simulate their spatial extent and hydrological processes is important for valuing wetlands' function. The purpose of this study is to dynamically simulate wetlands' hydrological processes and their feedback to regional climate in the Prairie Pothole Region (PPR) of North America, where a large number of wetlands exist. In this study, we incorporated a wetland scheme into the Noah-MP Land Surface Model with two major modifications: (1) modifying the sub-grid saturation fraction for spatial wetland extent; (2) incorporating a dynamic water storage to simulate hydrological processes. This scheme was tested at a fen site in central Saskatchewan, Canada and applied regionally in the PPR with 13-year climate forcing produced by a high-resolution convection-permitting model. The differences between wetland and no-wetland simulations are significant, with increasing latent heat and evapotranspiration while decreasing sensible heat and runoff. Finally, the dynamic wetland scheme was tested using the coupled WRF model, showing an evident cooling effect of 1~3℃ in summer where wetlands are abundant. In particular, the wetland simulation shows reduction in the number of hot days for more than 10 days over the summer of 2006, when a long-lasting heatwave occurred. This research has great

implications for land surface/regional climate modeling, as well as wetland conservation, for valuing wetlands in providing a moisture source and mitigating extreme heatwaves, especially under climate change.

Plain Language Summary

A large number of wetlands exist in the Prairie Pothole Region (PPR) across U.S. and Canada. These wetlands are important to our environment as they can provide flood control and cool the temperature, but they are poorly represented in previous land surface model studies. In this study, we updated a dynamic wetland module in the Noah-MP land surface model to reasonably estimate wetland extent and seasonal variation in the PPR. This wetland module shows significant impacts to the surface energy and water balance and, hence, regional temperature. The results show that wetland features would effectively cool the air temperature 1~3 ℃ in summer, especially for regions with high wetland coverage. The implication of this study is very useful for wetland conservation agencies and climate scientists, as this cooling effect could potentially mitigate heat stress under climate change.

1 Introduction

Wetlands are important and unique ecosystems that play vital roles in Earth's ecosystem balance and biodiversity. Although wetlands occupy a small portion of the global land surface (~6%), they store about one third of terrestrial carbon (Lehner and Döll, 2004; Mitra et al., 2005; Mitsch and Gosselink, 2007). Moreover, due to their unique productivity, wetlands support a wide variety of plants, birds, and amphibians, and are areas of high biodiversity (The Ramsar Convention, 2007). Wetlands are natural reservoirs to prevent flooding, especially in high latitude and mountainous regions (Hayashi et al., 2016; Pattison-Williams et al., 2018). After springtime snowmelt or heavy rainfall, surface runoff can be stored in wetlands, effectively reducing the peak flow and delaying the peak time of flooding, hence, mitigating flooding impacts. From a climate regulation perspective, the presence of surface water and the moisture of wetland soils can effectively store surface energy and favor energy partitioning to latent heat flux over sensible heat. Specifically, greater partitioning of latent heat flux over sensible heat flux in wetland water bodies decreases summer temperature (Bonan, 1995) and reduces daily air temperature variability (Hostetler et al. 1993). This land-atmosphere interaction is analogous to the soil moisture-temperature feedback (Seneviratnes et al., 2010), inducing a cooling effect to surrounding environments.

The North American Prairie Pothole Region (PPR contains millions of small wetlands, known as "potholes", due to its unique geology, hydrology, and climate conditions. The retreat of continental ice sheets over 11, 000 years ago left glacial deposition upon the landscape, forming millions of depressions. These depressions are isolated from large river networks and are poorly hydraulically connected. The cold winters allow snow to accumulate over cold seasons, and springtime runoff and seasonal rainfall are major water inputs to these wet-

2

lands. Over the warm season, evaporation exceeds precipitation, drying surface water and exposing the underlying soils. The persistence and storage of wetland ponds depend on receiving seasonal rainfall and connection with shallow groundwater. Under extremely wet conditions, strong rainfall or sudden snowmelt increases the water level of wetlands, exceeding the maximum capacity. Several filled wetlands will spill water to other surrounding wetlands, a "fill-and-spill" process, and form a largely connected wetland complex (van der Kamp and Hayashi, 2009; Mekonnen et al., 2014; Vanderhoof et al., 2018). These complex interactions between climate, wetland, and groundwater make it challenging to simulate in traditional hydrological models and land surface models (LSMs).

Given their importance to global and regional environments, the need to represent wetland physics in earth system models (ESMs) and LSMs has emerged in recent decades. In the Community Land Model (Oleson et al., 2008) and Noah-MP LSM (Niu et al., 2011; Yang et al., 2011), a relationship has been established between grid cell saturated fraction and the depth of groundwater, based on the TOPMODEL hydrological model (Beven and Kirkby, 1979) and its application in LSMs (Famiglietti and Wood, 1991, 1994a). This method assumes the sub-grid representation of grid cell saturation is based on a redistribution of water table depth, given the variation of slope and contributing areas in the grid cell. A sub-grid saturated fraction F_{sat} is defined for the local water table at the surface and can be used for runoff generation as saturationed excess runoff. While this may be sufficient estimation over a large grid resolution in many GCM models (~50-100 km), it is not sufficiently detailed for high-resolution regional simulation (~5-10 km). Despite its limitations, TOPMODEL- based F_{sat} is widely used in many LSMs and ESMs, particularly in representing global wetland extents. The discrepancies in projecting wetland extents have significant implications for modeled CH_4 emissions, as summarized in a wetland CH_4 inter-comparison modeling project (WETCHIMP, Wania et al., 2013, Melton et al., 2013).

On the other hand, many models have incorporated surface water storage schemes to represent the dynamics of lakes and wetlands to investigate their impacts on the energy and water cycles. For example, Pitman (1991) incorporated a sub-grid scheme for water surfaces and their contribution to latent and sensible heat as the weighted average over the fraction of water, vegetated and bare ground surface in a coarse resolution (~2°) GCM. The Variable Infiltration Capacity model (VIC, Liang et al., 1994) has developed a dynamic lake and wetland scheme to study the impacts of surface water heterogeneity on energy and water balance (Bowling and Lettenmaier, 2010). Results show that incorporating wetlands increases the annual ET by 5% and decreases runoff by ~ 12% in the U.S. Midwest region. Latent heat fluxes also increase, with corresponding decreases in sensible heat fluxes . Despite robust results in surface energy and water balance, this research is not coupled with regional climate models, therefore omitting the feedback from wetlands to temperature and precipitation.

3

The purpose of this study is to quantify the impacts of wetlands on the surface energy and water balances, as well as their feedback to regional climate in a high-resolution convection-permitting regional climate model (CPRCM, Prein et al., 2015). For this purpose, we have established three steps: (1) Develop a physical process-based parameterization of sub-grid wetland extent and a dynamic wetland storage scheme; (2) Explore the impacts of inclusion of this wetland parameterization on the surface energy and water balance in offline regional land-surface hydrology simulations using Noah-MP; (3) Investigate the interactions between the wetland hydrological cycle and its feedback to regional climate using a coupled Weather Research & Forecasting (WRF, Skamarock et al., 2019) and Noah-MP model system. In particular, we want to investigate the potential cooling effect of surface wetlands in mitigating summertime heat stress, especially during the widespread high-intensity heatwave of 2006 in Southern Canada and the U.S.

2 Materials and Methods

2.1 Global Inundation Extent from Multiple Satellites (GIEMS-2)

The 1993-2007 Global Inundation Extent from Multiple Satellites (GIEMS-2) is a unique dataset that provides estimates of surface water extent and dynamics, based on a collection of satellite observations (https://lerma.obspm.fr/spip.php?article91&lang=en). The satellite data are used to calculate monthly-mean inundated fractions of equal-area grid cells (0.25°x0.25° at the equator), taking into account the contribution of vegetation (Prigent et al., 2001, 2007, 2012; Papa et al., 2010). Such estimates use both passive and active microwave measurements, along with visible and near-infrared reflectance to capitalize on their complementary strengths, to extract maximum information about inundation characteristics, and to minimize problems related to one instrument only. The technique is globally applicable without any tuning for particular environments. The GIEMS data have been widely used to evaluate surface wetland extents in multiple GCM intercomparison studies for simulating wetland extents (Wania et al., 2012; Melton et al., 2012).

2.2 Convection-permitting regional climate simulation

Convection-permitting models (CPMs) are atmospheric models whose grid spacing is fine enough (usually < 5-km) to permit convection and resolve mesoscale orography (Rasmussen et al., 2011; Prein et al., 2015; Liu et al., 2017). Long-term high-resolution climate downscaling using CPMs provides important added value to improve precipitation forecasts, which is critical to surface wetland hydrology, as well as for resolving fine-scale land surface heterogeneity (Kenden et al., 2017).

The WRF convection-permitting regional climate simulation over the Contiguous U.S. (CONUS WRF, Liu et al., 2017) provides the opportunity for long-term (13-year), high-resolution (4-km) land surface modeling (Zhang et al., 2020). The CONUS WRF consists of simulations for the current climate and for future climate using the Pseudo Global Warming (PGW) method (Schär et al.,

1996, Rasmussen et al. 2011). The current climate simulation is a retrospective run from 2000-10-01 to 2013-10-01, forced by ERA-Interim (Dee et al., 2011) as boundary and initial conditions. For the future simulations, a delta climate perturbation, derived from the 19-model ensemble in the CMIP5 project under RCP8.5 scenario at the end of the 21st century, is added upon the ERA-Interim forcing. The future simulation represents an equivalent 13-year period at the end of the 21st century. The CONUS WRF forcing has been used in multiple climate, hydrology, and land surface studies (Zhang et al., 2020; Fang et al., 2021). In this study, we use CONUS WRF forcing in the PPR for offline land-surface model regional simulations to study the impacts of incorporating a surface wetland scheme on the regional energy and water balance in the PPR.

2.3 Application of TOPMODEL in LSMs

TOPMODEL (TOPography based hydrological MODEL) is a rainfall-runoff model that uses topography data to reflect dynamic process response in downslope hydrology, especially in runoff generation on variable contributing areas (Beven and Kirkby, 1979; Beven et al., 2020). Its basic assumption is that the runoff generation response to steady state rainfall is proportional to the spatial variation of moisture content in a drainage basin and can be characterized by its topographic variation, characterized by digital topography analysis. In the model, a topographic index is defined, $\Lambda = ln(\frac{a}{\tan})$, where a is the area draining through a point from upslope and tan is the local slope angle. High index values are likely to saturate first, hence, they indicate potential subsurface or surface contributing areas (Beven, 1997).

The simplicity of the model comes from the assumption that all the points of the same value of the index respond similarly in the catchment. Therefore, it is not necessary to calculate all the points in a catchment, but rather to integrate the hydrologic response of each interval of index values in a representative distribution function. At steady state, a critical threshold value for the local topographic index (Λ_{cri}) can be obtained when local water table depth is at the surface, compared to the grid cell mean water table depth. Hence, a sub-grid fraction F_{sat} can be defined by integrating the topographic index interval from this critical value to the maximum, following its probability distribution function:

$$F_{sat} = \int_{\Lambda_{cri}}^{\infty} pdf(\Lambda)d\Lambda \quad (1)$$

This probability distribution function was assumed to be a three-parameter gamma distribution by Sivapalan et al. (1987).

This F_{sat} fraction is an important parameter in partitioning surface water using the saturation runoff mechanism, i.e., the F_{sat} portion of the surface water from rainfall and snowmelt becomes surface runoff and the remaining (1-F_{sat}) becomes infiltration. The sub-grid F_{sat} is also critical in controlling surface energy balance and land-atmosphere interactions (Famiglietti and Wood, 1994a&b). In Famiglietti and Wood (1994a&b), a Soil-Vegetation-Atmosphere Transfer

Scheme (SVATS) is applied at local-, catchment- and macro-scales to demonstrate the sub-grid soil moisture heterogeneity in controlling both evapotranspiration and runoff. The total evapotranspiration over the sub-grid topographic index in a grid cell is the integration of the potential evaporation from saturated portion to drier land surface outside the transitional region, where evapotranspiration is restricted by active vegetation and soil moisture (Famiglietti and Wood 1994a). This framework for incorporating TOPMODEL into LSMs (TOPLATS) was utilized in the NASA GISS land surface model (Stieglitz et al., 1997) and the NASA Catchment Land Surface Model (CLSM, Koster et al., 2000; Bechtold et al., 2018) among others.

Due to its computational simplicity, the F_{sat} fraction is also very popular to represent surface wetland extent in large-scale global models (Gedney and Cox, 2003; Ringeval er al., 2011). The temporal and spatial variation of F_{sat} is based on groundwater dynamics interacting with soil moisture, simulating the expansion and shrinkage of surface wetlands. Although the meaning of saturation is not necessarily the same as inundation of wetland soils, this fractional area to some degree reflects the wetness conditions in a given grid cell, as well as its function partitioning surface water in "saturation excess" runoff generation. Thus, it has been widely applied in various LSMs and multiple modeling studies simulating wetland extents (WETCHIMP, Wania et al., 2013; Melton et al., 2013).

In the Noah-MP LSM, the energy balance is calculated separately for two sub-grid semitiles: a fractional vegetated area (F_{veg}) and a fraction bare ground area (1-F_{veg}). In this semitile scheme, shortwave radiation transfer is computed over the entire grid, while longwave radiation, sensible and latent heat flux, and ground heat flux are computed separately over these two tiles. As such, these two tiles in a Noah-MP grid neglect the large extent and seasonal variability of open-water wetlands. The total latent (LH) and sensible heat (SH) of these two semitiles are aggregated in a weighted function:

$LH = F_{\mathrm{veg}} \left(\mathrm{LE}_{\mathrm{gv}} + \mathrm{LE}_v\right) + (1 - F_{\mathrm{veg}})\mathrm{LE}_{\mathrm{gb}}$ (2)

$SH = F_{\mathrm{veg}} \left(\mathrm{SH}_{\mathrm{gv}} + \mathrm{SH}_v\right) + (1 - F_{\mathrm{veg}})\mathrm{SH}_{\mathrm{gb}}$ (3)

Where the subscript v represents the vegetation canopy, gv is ground under canopy and gb is the bare ground flux.

Additionally, the TOPMODEL-based runoff generation model is utilized for surface water partitioning: F_{sat} portion of the surface available water (Q_{insurf}) from snowmelt or precipitation becomes surface runoff (R_{srf}) and (1-F_{sat}) portion becomes infiltration (Q_{infil}). In Niu and Yang (2005), the probability distribution function of F_{sat} in equation (1) is replaced by an exponential function of the water table depth (Z_{∇}, equation (6)) and has been utilized in both CLM (Oleson et al., 2008) and Noah-MP LSM (Niu et al., 2011; Yang et al., 2011). F_{satmx} is the maximum saturated fraction in a grid cell derived from digital elevation model (DEM).

6

$R_{\mathrm{srf}} = Q_{\mathrm{insurf}} * F_{\mathrm{sat}}$ (4)

$Q_{\mathrm{infil}} = Q_{\mathrm{insurf}} * (1 - F_{\mathrm{sat}})$ (5)

$F_{\mathrm{sat}} = F_{\mathrm{satmx}} * exp(-0.5 * f * (Z_{\nabla} - 2))$ (6)

However, the above water balance setting does not reflect dynamic water movement in prairie wetlands. These wetland depressions actively receive surface water from snowmelt and rainfall, but there is no surface water storage process in Noah-MP, so that the simulated surface runoff component will leave the model grid. Additionally, this setting further neglects evaporation from the wetland surface to the atmosphere and discharge to surrounding wetlands in the fill-and-spill process. Therefore, a dynamic surface wetland storage scheme, incorporating both sub-grid energy and water balance, is needed to represent the complex hydrological processes in the prairie wetland landscape and their potential feedback to the atmosphere.

2.4 Modifying F_{sat} fraction to represent wetlands

The original TOPMODEL-based F_{sat}, based on an exponential function of water table depth, does not reasonably reflect the magnitude and seasonal variation of wetland extent in the Prairies. Figures 1 and 2 show the spatial distribution and temporal evolution of the inundation fraction from GIEMS and Noah-MP simulated F_{sat} fraction in the PPR region from 2000 to 2014. It is clear that the modeled F_{sat} has underestimated the maximum extent while overestimating the minimum extent. This is because of two reasons: (1) the parameter F_{satmx} is a fixed value (0.38) for the global mean; and, (2) the seasonally frozen soil and glacial till with low hydraulic conductivity prevent direct groundwater connection with surface water, hence the water table dynamic is not a good indicator of surface water extent in the PPR. Detailed reasons for this discrepancy are provided in the discussion section.
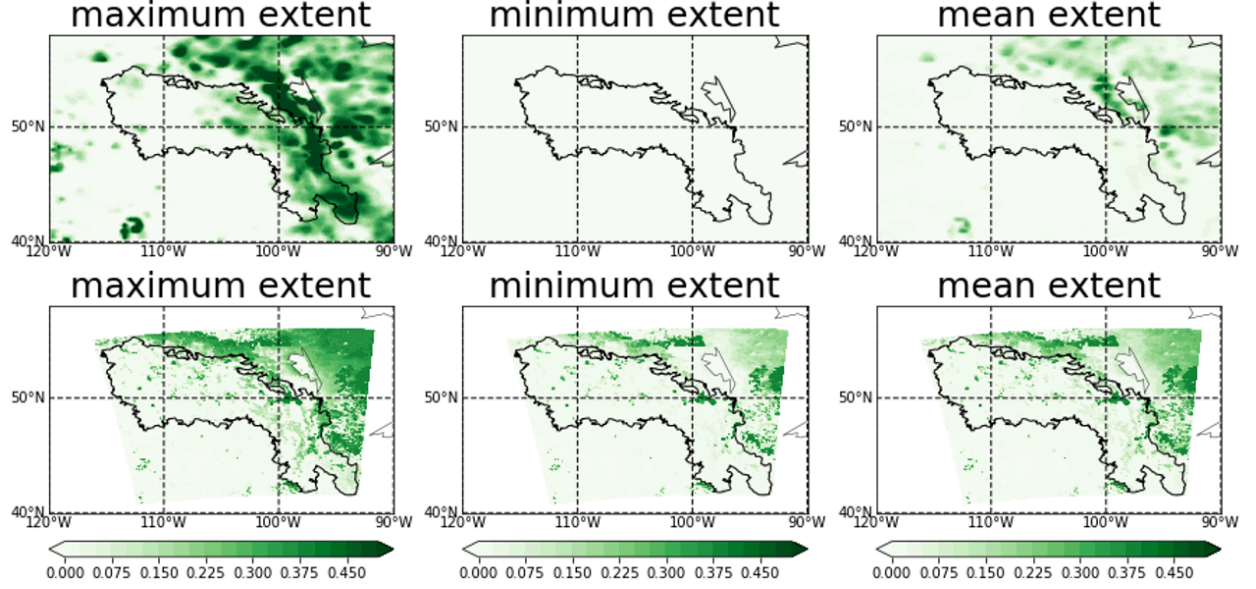
Figure 1. Spatial distribution of surface water extent from GIEMS (top) and Noah-MP modeled F_{sat} (bottom) in the Prairie Pothole Region (black outline).
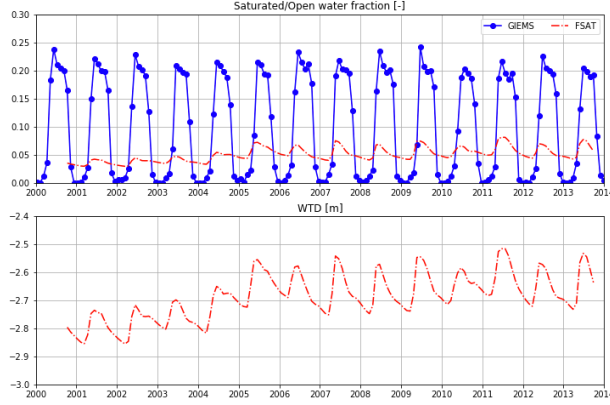

Figure 2. Temporal evolution of the inundation fraction from GIEMS and Noah-MP modelled F_{sat} in the Prairie Pothole Region.

Therefore, we propose a new formula for the saturated fraction F_{sat}, based on the first layer soil saturation, instead of water table depth:

$$F_{\text{sat}} = F_{\text{satmx}} * \left(\frac{SH_2O - \text{SM}_{\text{wlt}}}{\text{SM}_{\text{ref}} - \text{SM}_{\text{wlt}}} \right) \ (7)$$

The first layer soil moisture (SH_2O) responds more rapidly to surface hydrological processes, such as snowmelt infiltration and evapotranspiration, than groundwater level. F_{sat} is determined by the maximum saturated fraction (F_{satmx}) and a relative soil moisture saturation condition, normalized by the soil mois-

8

ture wilting point (SM_wlt) and field capacity (SM_ref). This assumes the mean soil moisture saturation in the first layer soil can empirically represent spatial heterogeneity of soil saturation at the sub-grid scale.

2.5 Implementing the surface wetland storage scheme

In this study, we incorporate a sub-grid bucket-style surface water storage scheme to represent the surface water dynamics in Prairie Pothole wetlands in North America by capturing three important processes in its water balance: (1) wetland storage receives water from snowmelt runoff and rainfall; (2) water in wetland storage would evaporate at the potential rate, calculated using the Penman equation in equation (10); (3) when the water exceeds the wetland maximum storage capacity (W_cap), it will spill out and become the outflow term. This wetland storage scheme operates at the sub-grid scale and uses F_sat to determine the inflow of water input from precipitation and snowmelt and contributes to the latent heat flux as a weighted average over all three sub-grid types, similar to the treatment in Pitman (1991). The sensible heat flux is calculated as the residual term from the energy balance equation.

$$Q_\text{insur} = Q_\text{snowmelt} + Q_\text{rain} \ (8)$$

$$Q_\text{inflow} = Q_\text{insur} * F_\text{sat} \ (9)$$

$$Q_\text{evap} = \frac{m R_n + \rho c_p (\ e) g_a}{\lambda_v (m + \gamma)} \ (10)$$

$$\text{LH}_\text{all} = (1 - F_\text{sat})(F_\text{veg}\left(\text{LE}_{g,v} + \text{LE}_v\right) + (1 - F_\text{veg})\text{LE}_{g,b}) + F_\text{sat} * Q_\text{evap}\lambda_v (11)$$

$$Q_\text{outflow} = max(Q_\text{inflow} - W_\text{cap}, 0) \ (12)$$

$$W_\text{surf} = Q_\text{inflow} - Q_\text{evap} * F_\text{sat} - Q_\text{outflow} \ (13)$$

In many traditional LSM treatments, surface runoff is treated as a drainage term that leaves the grid cell and is lost to the water balance. In our new scheme, the surface runoff from snowmelt and rainfall becomes the inflow to surface water storage (Q_inflow). The water in surface wetlands evaporates to the atmosphere at the potential rate, calculated by the Penman equation. The outflow is a result of total water exceeding the maximum water storage (W_cap), characterizing the "fill-and-spill" process. Note this surface wetland storage scheme is not connected to other wetland storage or a river network, so that the outflow term will leave the grid point and is lost to the water balance, as parameterized in the default Noah-MP. The change of surface water storage (W_surf) is calculated by the net balance of inflow, evaporation, and outflow.

Figure 3 illustrates the difference between the default Noah-MP and the modified surface runoff scheme in this study. The left-hand side shows the default Noah-MP surface runoff scheme based on the TOPMODEL saturation-excess concept. The inflow from rain and snowmelt (Q_insur) will be partitioned into infiltration (in the 1-F_sat portion), which enters soil moisture, and to surface runoff (in the F_sat portion), which eventually leaves the grid cell. The right-hand

side shows the two modifications in our study: (1) the modified F_{sat} parameterization based on first layer soil saturation; (2) creating a surface water storage W_{cap} representing surface wetland dynamics. The F_{sat} portion of the inflow will now be collected within the W_{cap} storage and evaporate to the atmosphere with a weighted function. The water amount exceeding the maximum capacity will become the outflow from the wetland (also referred to as the new runoff term, R_{srf}).
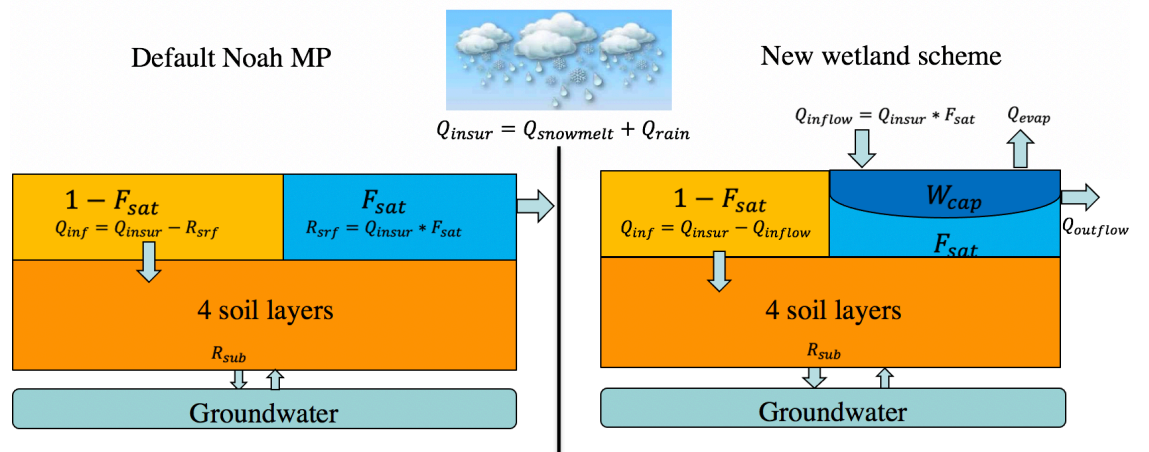
Figure 3. Simple diagram demonstrating the modifications in this study, which includes the modification of surface saturated fraction and incorporating a surface wetland storage scheme in the Noah-MP Land Surface Model.

2.6 Simulation design

Three sets of numerical simulations are conducted to study impacts of representing wetlands on the simulated energy and water balance in the Noah-MP LSM, as well as feedback to the regional climate in the coupled WRF system. A summary of these three simulations is in Table 1.

The first set of simulations is a single-point test, driven by observed forcing, in a half-water/half-vegetation fen site in central Saskatchewan. This is to study the impacts of modifying the F_{sat} parameterization and the sensitivity of dynamical storage and its impacts on the energy/water balance.

The second set of simulations is on the regional scale in the PPR, driven by a 4-km WRF regional climate simulation (CONUS WRF, Liu et al., 2017). In this simulation, we constrain the maximum F_{satmx} by satellite observation data (GIEMS) and combine the surface water storage with fine-scale 90-m DEM (MERIT data:http://hydro.iis.utokyo.ac.jp/~yamadai/MERIT_DEM/). The purpose of this offline simulation is to investigate the implementation on a regional scale, with respect to spatial heterogeneity of F_{satmx} and W_{cap}.

The third set is the coupled WRF regional climate simulation for three summers

with strong inter-annual variability: 2005 (wet), 2006 (dry), and 2007 (normal). This is to study the impacts of surface wetland dynamics and their feedback to regional climate, in particular under a high-resolution convection-permitting configuration. It is also noteworthy that in the summer of 2006, an intense and prolonged heatwave occurred in the Central U.S. and Southern Canada from mid-July to early August.

Table 1. Summary of the three simulations conducted in this study.

Simulation design	Location	Period	Purpose
Single-point Noah-MP	Fen site, SK	2003/01/01-2010/12/31	Exam the sensitivity
Offline regional Noah-MP	PPR region	2000/10/01-2013/10/01	Incorporate spatially
Coupled regional WRF	PPR region	2005-2007, three summers from Apr to Aug	Conduct coupled W

3 Results

3.1 Implementation and sensitivity tests on a single-point LSM

We first performed a single-point LSM simulation in the fen site in North Saskatchewan. Two modifications were tested: first, the modified F_{sat} formula and, second, a sensitivity test for surface water dynamics with various storage capacities. Figure 4 shows the F_{sat} parameter, energy and water balance in the fen site simulated by Noah-MP. In Figure 4a, the default F_{sat} formula using the exponential function of the water table depth fails to represent the large magnitude and strong seasonal variation, as shown by the GIEMS data. The modified formula using the first layer of soil moisture improves both the magnitude and seasonal cycle of the F_{sat} parameter. This larger F_{sat} effectively changes the surface water partitioning, by increasing the surface runoff, which leaves the grid point water balance, and reducing the infiltration to soil moisture, which further reduces ET and underground runoff (Figure 4b). Furthermore, the increased F_{sat} reduces latent heat fluxes and enhances sensible heat fluxes from March to September, with the strongest decrease in July (Figure 4c).

The surface wetland scheme (Section 2.4) collects the increased surface runoff in wetland storage and allows evaporation to the atmosphere. The scheme's contribution to surface water and energy balance depends on its storage capacity. Figure 4d shows the sensitivity of water storage in a wetland with four different capacities (WS=0, 5, 50 and 500 mm). When wetland storage = 5 mm ("WS=5"), the wetland water would be depleted during the summer, while with larger capacity (WS=50 or 500), the water storage from the previous year can be sustained through dry seasons. Greater water-holding capacity allows greater contribution to evaporation and reduces surface runoff (Figure 4e). The changing storage capacity has little impact on underground runoff. Moreover, greater storage capacity also allows greater latent heat flux and less sensible heat flux. The effect threshold lies between WS=5 and WS=50, as water may be dried in smaller capacities, while the contribution is similar between WS=50 and WS=500.
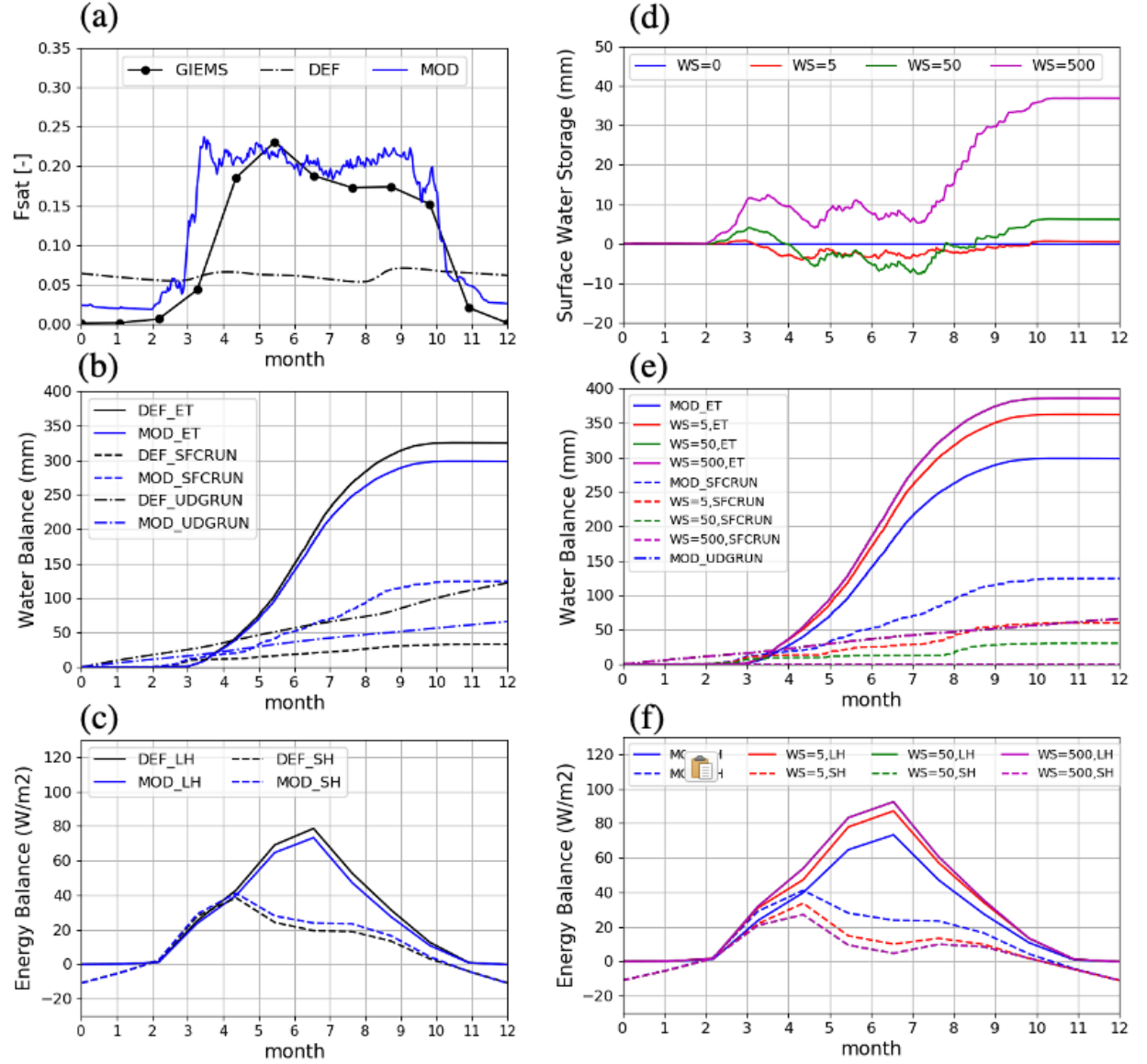
11

Figure 4. Single-point simulation of F_{sat} modification (a-c) and incorporation of dynamic wetland storage (d-f) in a fen site in central Saskatchewan: (a) surface saturated fraction from default (DEF) and modified (MOD) formula and GIEMS inundation extent, (b) surface water balance in ET, surface and underground runoff, (c) surface energy balance in sensible and latent heat fluxes; (d) water level change with variable levels of wetland storage, (e) surface water balance in ET, surface and underground runoff, (f) surface energy balance in sensible and latent heat fluxes.

3.2 Regional-scale land model simulation constrained by spatially varied parameters

To simulate wetland dynamics at regional scales, it is essential to constrain two spatially varied parameters, F_{satmx} and the storage capacity, W_{cap}, as they are critical to wetland energy and water balance shown in the last section. Figure 5 shows the spatial map of F_{satmx} and W_{cap} in the PPR. Here, F_{satmx} is derived from the GIEMS inundation fraction to represent the sub-grid maximum saturation, and W_{cap} is derived from the MERIT 90-m DEM and aggregated to a 4-km resolution grid (same resolution as in CONUS WRF meteorological forcing).

$$W_{cap} = \sum_{i=1}^{n} min((H_i - \overline{H}), 0) \quad (14)$$

H_i represents the 90-m elevation and $\overline{H}$ is the mean elevation for a 4-km grid, such that W_{cap} represents the collective topographical variation in the depressional area from 90-m DEM and aggregated into the 4-km grid.
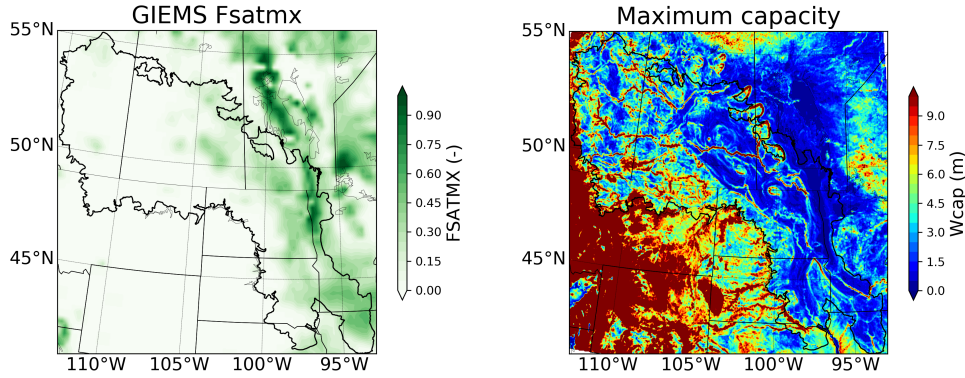
Figure 5. Map of maximum saturation (F_{satmx}) and wetland storage capacity (W_{cap}) in the Prairie Pothole Region, derived from the Global Inundation Extent from Multiple Satellites (GIEMS) product and MERIT 90-m DEM, respectively.

The high F_{satmx} regions are located in the Northeast part of the domain, near Lake Winnipeg in Manitoba and the Red River Valley. These regions also correspond with the low W_{cap} regions.

Two 13-year offline Noah-MP simulations were conducted: one with the default setting and one with the new wetland scheme. The 13-year average surface water balance (surface runoff and ET) and energy balance (sensible heat and latent heat) are shown in Figure 6. Figure 6a shows substantial wetland water storage availability – more than 200 mm average over the summer months, in the north domain and in the southeastern PPR in the Red River valley. In the central and western PPR, wetland storage is generally less than 100 mm, with some deeper storage in large water bodies surrounding lakes and rivers.

13

The surface water and energy balance in the PPR are greatly altered by the presence of surface wetlands and the differences between WS and DEF simulation follow their spatial distribution. The presence of surface wetlands generally holds inflow water from rain and snowmelt, reducing surface runoff while increasing evaporation by about 100~200 mm in summer months. The water in the saturated fraction of the grid cell creates an open water surface, reducing (increasing) the sensible (latent) heat fluxes by about 0~50 W/m2 in summer months. These impacts on surface energy and water compensate for each other, and the presence of open water storage may induce potential feedback to the atmosphere through land-atmosphere interactions, which we will discuss in next section.

Wetland map shows large storage (greater than 200 mm) in North and East of the PPR. In West PPR less than 100 mm (shallow)
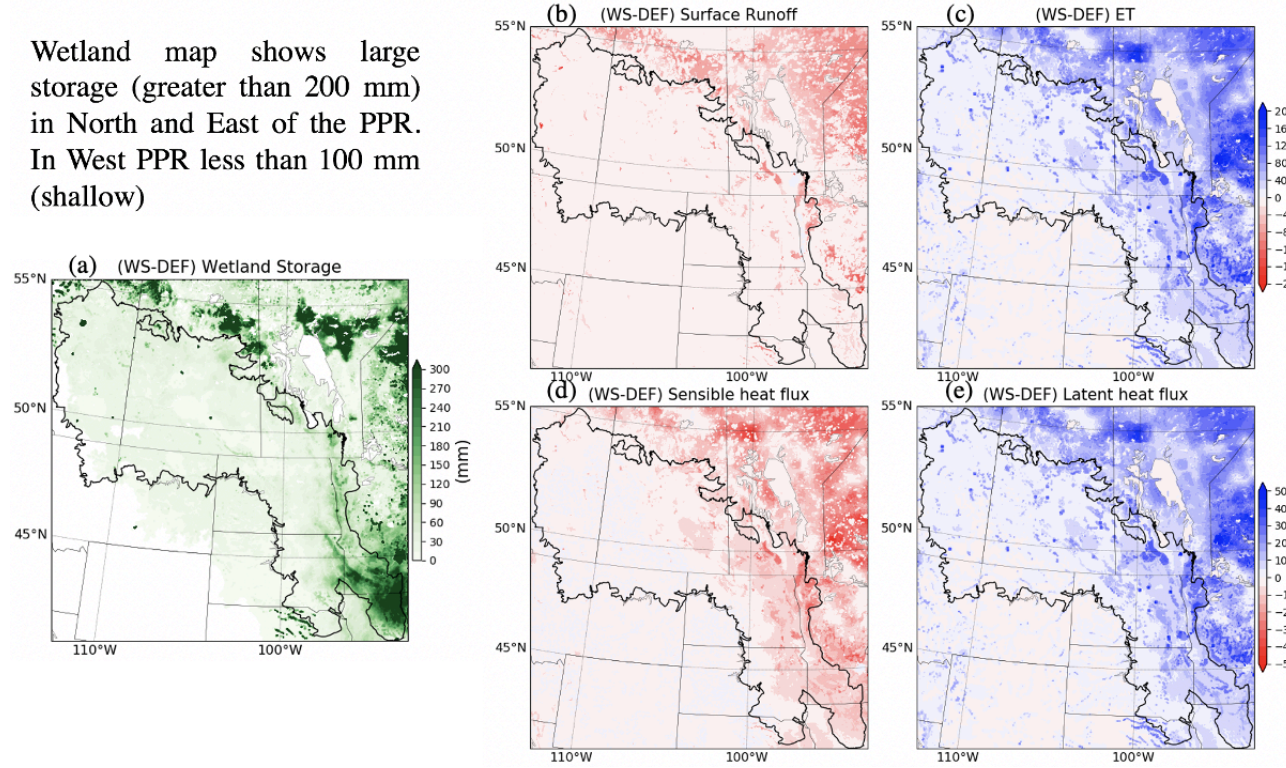
Figure 6. 13-year summertime (MJJA) mean wetland storage level (a); and difference between wetland storage (WS) and default (DEF) simulations in surface runoff (b), evapotranspiration (ET, c), sensible heat flux (d), and latent heat flux (e).

3.3 Regional climate simulation with coupled wetland dynamics

To study the feedback from wetlands to regional climate, we performed two coupled WRF-wetland simulations for the summers of 2005, 2006, and 2007. The first, default (DEF) simulation includes the shallow groundwater scheme

from Miguez-Macho et al. (2007). The second simulation (WS simulation) incorporates the wetland scheme upon the shallow groundwater scheme. These simulations start from April and run through August, with the first month as the spin-up period. Our analysis focuses on the temperature and precipitation from May to August for these three years, especially in 2006 when an intense summer heatwave occurred from mid-July to early August in the Central U.S. and Southern Canada.

Figure 7 shows the monthly temperature from station observation, model biases from two simulations, and the cooling effect induced by the WS scheme in 2006. It is clear that a warm bias exists in the southern part of the domain, ranging from 2℃ in the Central U.S. to 1℃ in the Western Canadian Prairies. This warm bias is particularly getting stronger in July and August. The WS simulation shows a significant cooling effect in the Northeast portion of the domain, where the saturated fraction is high. The cooling in temperature ranges from less than 1℃ in May to about 1~2℃ in July. This cooling signal is evident in high-Fsat regions in the domain in all three-year simulations.
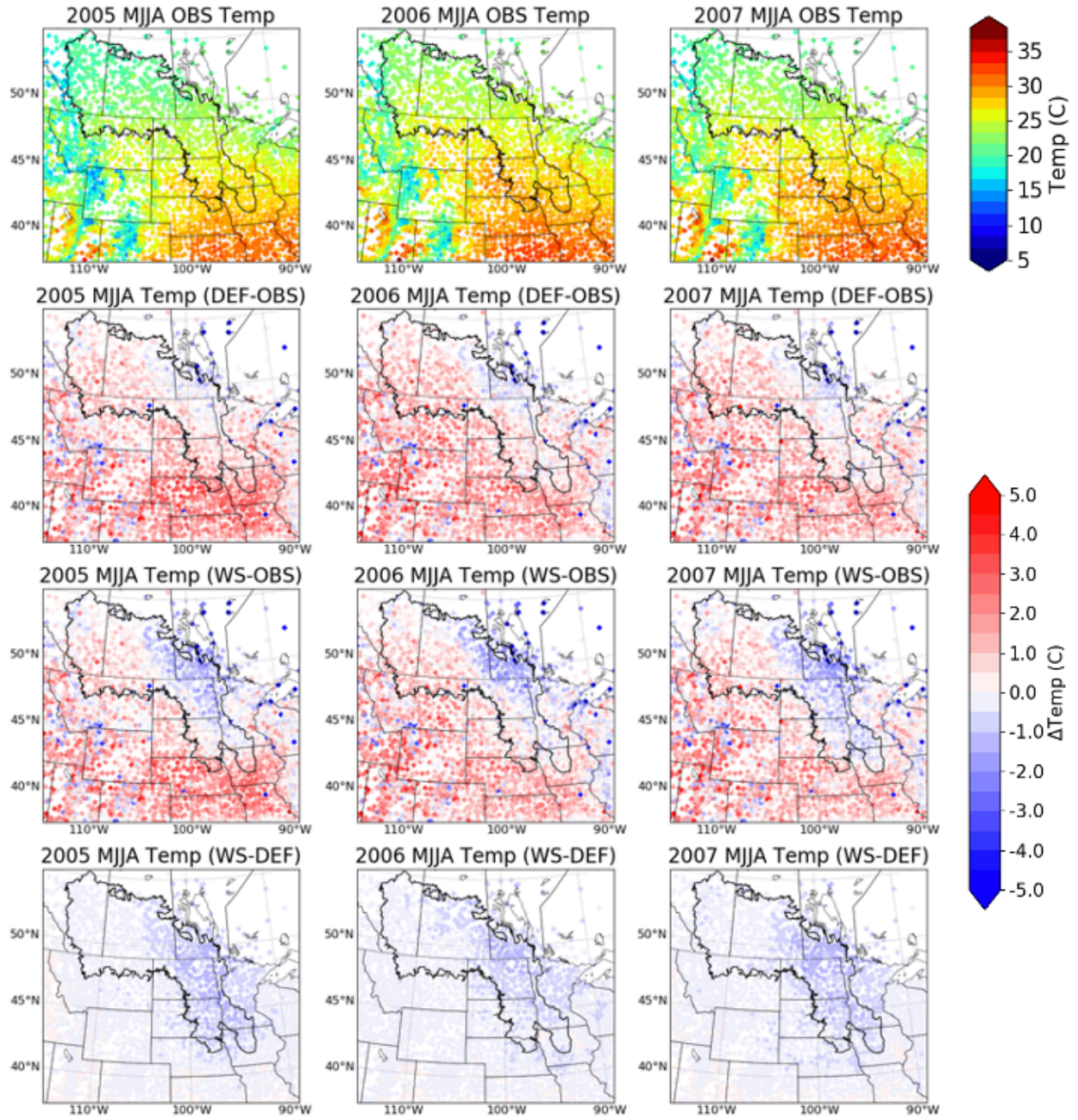
Figure 7. Monthly temperature from station observation, temperature biases from default (DEF) and wetland scheme (WS) simulations, and the cooling effect induced by the WS in the summer (May-August) for three-year simulations.

In the summer of 2006, a record-breaking heatwave hit the major part of the

U.S. and Southern Canada. The extreme heat conditions can be represented by the number of "hot days" during the summer, with the daily maximum temperature exceeding the 90th percentile of the 30-year climatology. We summed the number of hot days from May to August in 2006 from two simulations and the results are shown in Figure 8. Through these four months, the hottest region is in the southeast of the domain in Nebraska, Iowa, Kansas and Missouri – with more than 40 hot days – while in the Northern Great Plains and Canadian Prairies, the hot days are about 10~20 days. The WS simulation shows that wetlands could effectively reduce the number of hot days by about 10 days in the entire domain. Two regions receive greater impacts from wetlands, including southern Manitoba and the area between Nebraska and Iowa. This result manifests the important role of wetlands in mitigating climate change, especially in extreme heat events.
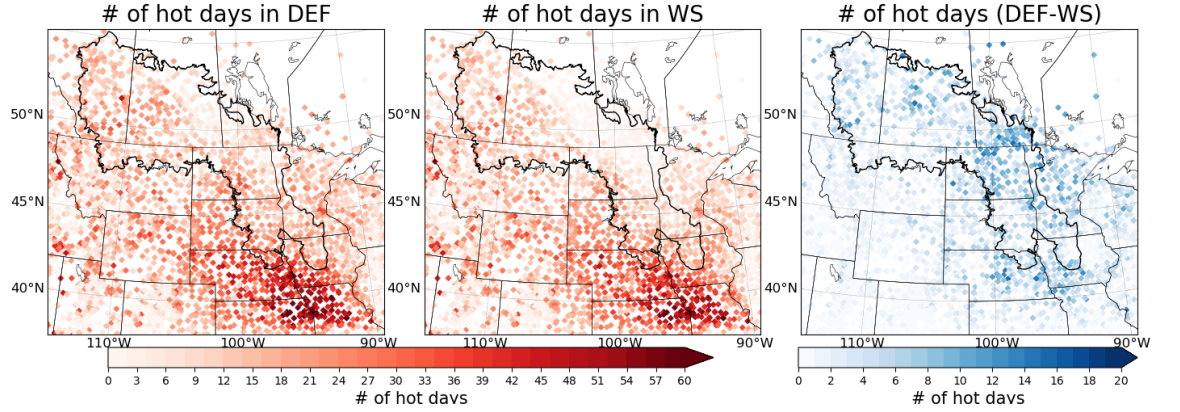
Figure 8. Number of hot days in default (DEF) and wetland scheme (WS) simulations and the reduction in hot days from WS to DEF.

Figure 9 shows the wetland cooling effect on temperature versus its maximum saturated fraction for the domain. The F_{satmx} parameter generally corresponds to highly saturated regions with high water availability. The cooling effect from wetlands is evident for almost every month in the simulation period and is stronger in June and July than in May and August. The strongest effect is shown in 2005 July of almost 1.5 ℃ cooler. There exists a linear relationship between F_{satmx} and TEMP, especially in 2005 and 2007 — the larger the F_{satmx}, the stronger the cooling effect is. This pattern is not as clear in 2006, indicating that the wetland cooling effect relies on the available water input from precipitation: under normal and wet conditions, the greater the F_{satmx}, the more water can be stored in wetland storage, the more surface energy partitioned into latent heat, hence the stronger the cooling effect. However, in the 2006 dry conditions, there is not sufficient precipitation to fill these wetlands, limiting the wetlands' cooling effects and evaporation, regardless of F_{satmx} values. This wetland cooling effect is analogous to the classic soil moisture-temperature feedback in land-atmosphere interactions (Senviratnes et al., 2010; Perkins, 2015).
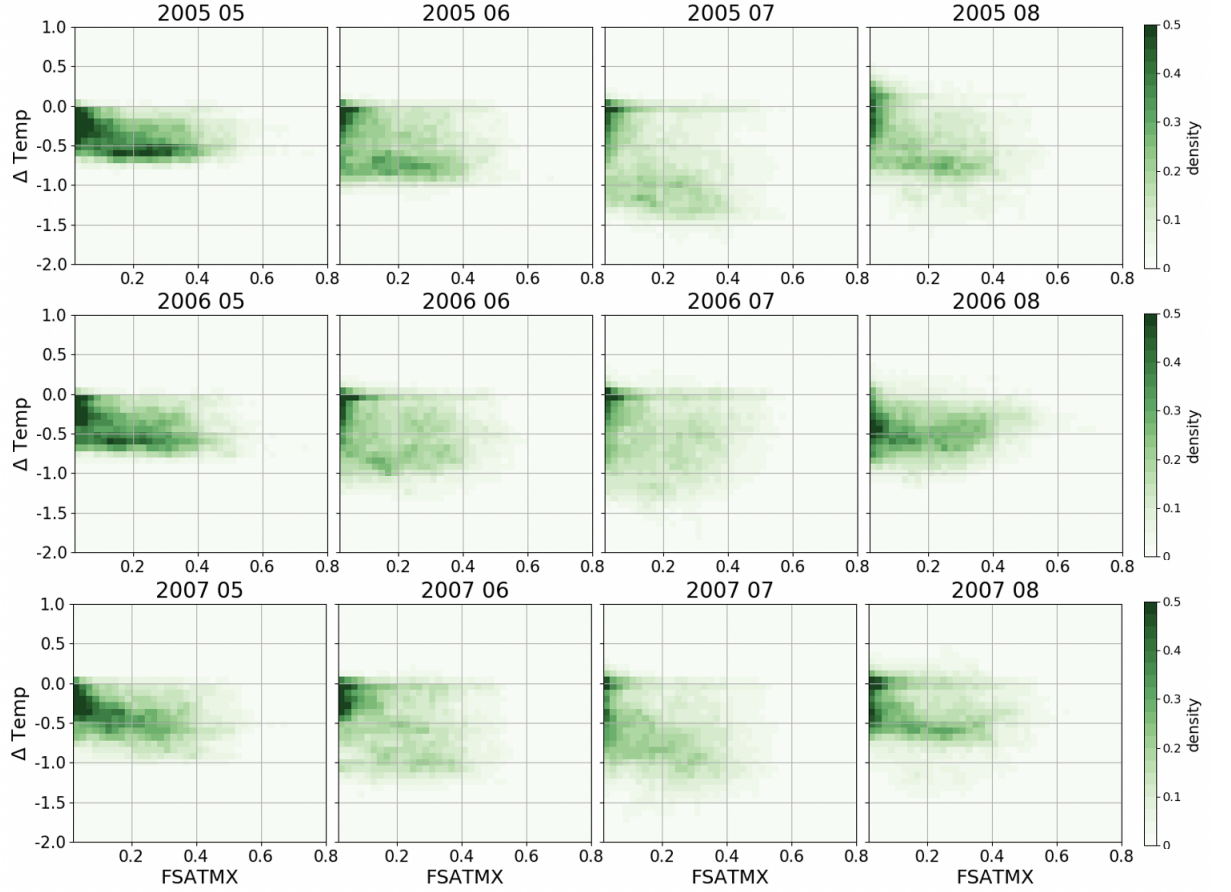
Figure 9. Scatter plot of TEMP (DEF-WS, ℃) against the F_{satmx}, maximum saturated fraction in grid cell, from three-year summer monthly data.

Compared to the uniform cooling effect on temperature, the feedback of wetlands to regional precipitation is more ambiguous. Figure 10 shows the monthly precipitation from observation, model biases from two simulations and their difference in three-year summers. The precipitation bias corresponds well with the temperature bias in Figure 7, with a significant dry bias in the southeast part of the domain while the precipitation is not as obvious in the Canadian Prairies. The WS simulations show little difference in precipitation from the DEF simulation and the signals of changes are almost random. This patchy precipitation signal is shown in all three-year simulations and for the accumulated period of four months.

18
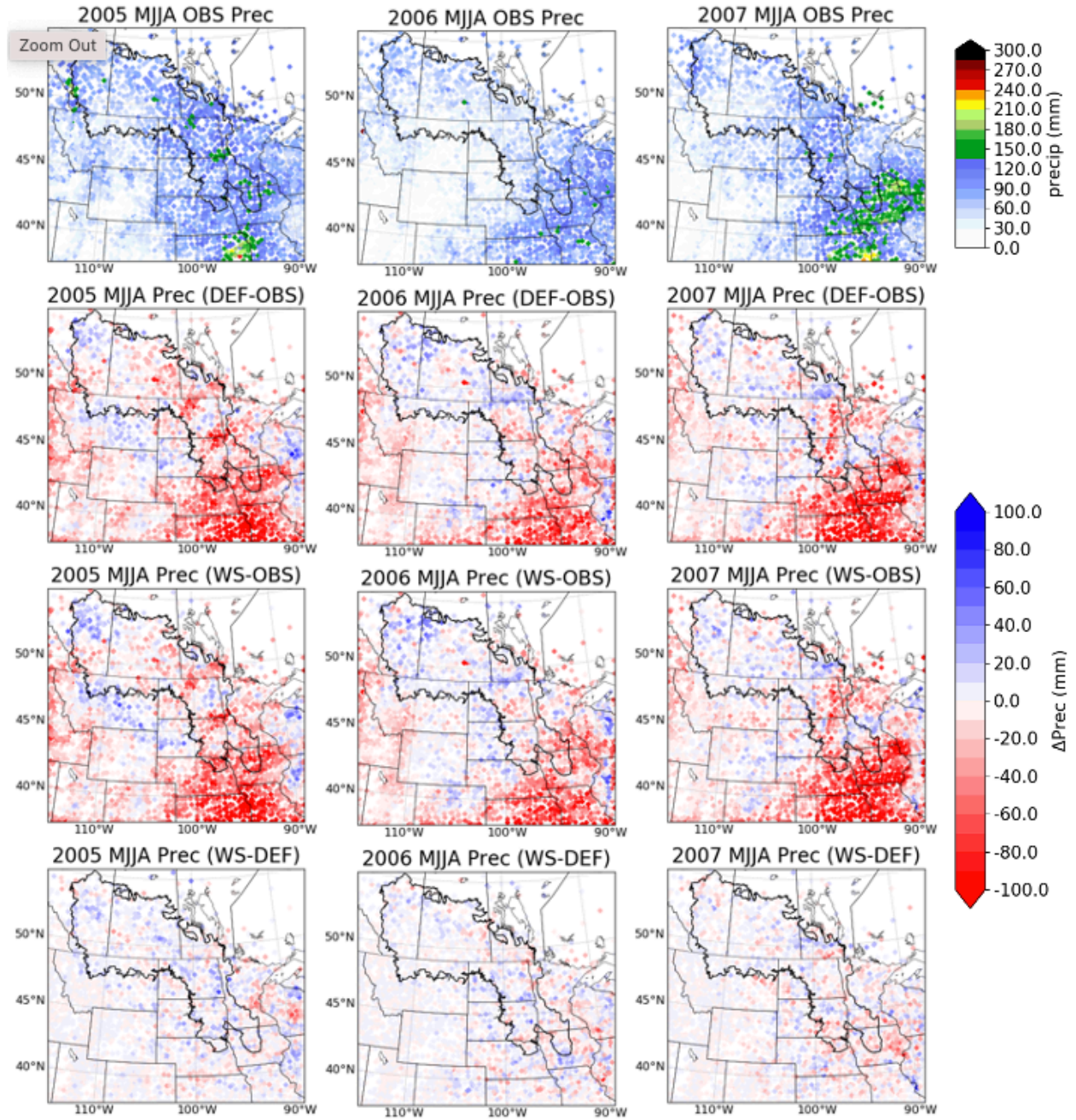
Figure 10. Monthly precipitation from station observations, precipitation biases from the default (DEF) and wetland scheme (WS) simulations, and the precipitation difference between WS and DEF simulations in the summer (May-August) for three-year simulations.

4 Discussion

LSMs and coupled ESMs, reasonable representations of wetland spatial extents and dynamic water storage are challenging in light of data scarcity, coarse model resolution, and insufficient understanding of the physical processes (Ringeval et al., 2012). However, because wetland extents play a key role in land-atmosphere interactions and carbon feedback to the climate system, researchers have long been interested in estimating wetland extents in hydrology-climate simulations from global to regional scales. For example, the WETCHIMP project gathered 10 participating GCMs for simulating global wetland extents and their CH_4 emissions (Wania et al., 2013; Melton et al., 2013). Many of these GCMs used prescribed wetland maps from global surveys or remote sensing products, such as the Global Lake and Wetland Database (Lehner and Döll, 2004) and GIEMS (Prigent et al., 2007), or used the TOPMODEL-based F_{sat} to simulate a subgrid "saturated" fraction to represent wetlands extents.

Although the TOPMODEL method can simulate some spatial heterogeneity and temporal dynamics of wetland extent, it generally underestimates both the maximum value and the seasonal variability. As we showed in Section 2.1, the TOPMODEL-based method in Noah-MP simulates a much lower F_{sat} value than the highly dynamic GIEMS product. Here we provide two possible reasons for the discrepancy between TOPMODEL F_{sat} and surface water dynamics from satellites. (1) The first underlying assumption of the TOPMODEL method requires "steady state" precipitation and soil moisture heterogeneity, which is more likely in wet, relatively shallow soils on moderate slopes (Beven and Kirkby, 1979; Kirkby et al., 2021). However, this is not the case in the Prairie Pothole Region, where the climate is usually semi-arid and the large-scale topography is flat with small-scale variation. (2) Another possible reason for this discrepancy is that the TOPMODEL method calculates a critical topographic index value when the local water table is at the surface; this value is used to determine the F_{sat} fraction through the integration of its probability distribution function. However, in the PPR, frozen soils in wintertime prevent interaction between the soil moisture and groundwater (Ireson et al., 2013). Therefore, in the TOP-MODEL method, the exponential function will simulate less seasonal variation in the surface water dynamics. A large portion of global wetlands and peatlands are located in high latitude regions where winter soil freezing is very common.

In our modification of the F_{sat} formulation, we used the first layer of soil saturation to indicate the sub-grid spatial extent of the saturated portion – the extent of wetlands. This method empirically assumes the grid cell mean soil moisture saturation can be translated into a spatial fraction for surface saturation and shows a highly variable F_{sat} value compared to the default TOPMODEL method, in terms of the maximum and minimum extent, and seasonality (Section 3.1). Moreover, we also incorporate a spatially varied maximum F_{satmx} map from the GIEMS product to replace the default global mean value (0.38) in Noah-MP and WRF. Both these modifications improve the spatial heterogeneity and the temporal dynamics of wetland extents in the PPR.

Additionally, we incorporated a dynamic surface water storage scheme to simulate the hydrological processes in wetlands. Although this scheme is simple, we aim to capture three important processes – the filling of wetlands by snowmelt and rainfall, the evaporation of wetland water into the atmosphere, and the excess water spilling to surface runoff. These three processes are the key components in the wetland water and energy cycle during the warm season open-water period. Our results showed increase of ET with a decrease of surface runoff and an increase of latent heat with decreases of sensible heat. This finding aligns with our expectations, as well as with previous VIC model wetland and lake simulations in the U.S. Midwest region (Mishra and Cherkauer et al., 2010).

Moreover, our scheme provides greater potential to explore wetlands' feedback to the atmosphere in coupled WRF-NoahMP-Wetland simulation. In the default simulation, which already includes the MMF groundwater scheme (Barlage et al., 2015, 2021), warm biases still exist at about 1~3 degrees in the U.S. Great Plains. Without the groundwater scheme, the summertime warm biases could be as high as 4~6 degrees. By adding the wetland scheme on top of the MMF groundwater scheme, the warm biases in the U.S. can be further reduced by 0.5~1.5 degrees, but it also introduces 1-degree cool biases in Southern Manitoba, where wetland extents are large. While the temperature cooling effect is evident, wetland feedback to precipitation is less clear and is more ambiguous. A previous study using WRF with a prescribed soil moisture threshold to indicate wetlands in the Great Plains at coarser resolution (12-km) also showed a temperature cooling effect, but the precipitation effect was negligible (Capehart et al., 2012).

One of the highlights of this study is the wetland cooling effect to the atmospheric temperature. Previous studies have documented this effect in detail, but they have been specific to different wetland characteristics and dominant vegetation types (Pitman, 1991; Bonan, 1995). In our study, we used general open-water storage to characterize wetland interactions with the atmosphere, omitting these variations in specific wetland types but gaining more generic conclusions in a much larger region. The wetland cooling effect on temperature, especially during extreme heatwave events, echoes a previous study in the Central U.S. where we found land surface characteristics could effectively reduce the frequency, intensity, and duration of extreme heatwaves (Zhang et al., 2018). However, more pronounced cooling occur in non-heatwave years (2005 and 2007) than in 2006, because the cooling effect also depends on water availability, hence, cannot be too dry.

In recent years, the tradeoffs between agriculture and wetland conservation has been a serious topic of discussion among the public, universities, and government agencies. It has been shown that the agricultural land expansion at the cost of wetland drainage increases the risk of emerging flooding in springtime (Dumanski et al., 2015; Pattison-Williams et al., 2018). Wetland drainage also results in increased nutrient export (Badiou et al., 2018; Wilson et al., 2019) and carbon release to the atmosphere (Badiou et al., 2011). This study suggests that the loss of wetlands for croplands also reduces resilience to drought and

high temperature, which may cause crop failures due to water and heat stress (Hatifield, 2016).

However, the loss of wetlands to agricultural, industrial and residential land is not confined to the PPR but are common problems worldwide and require humans' attention (The Rasmar Convention 2007; Nature Geoscience, 2021). These land use modifications not only threaten the local environment but also contribute to the global carbon balance and eventually cause problems for human beings. Understanding the effects of development is challenging. It is hoped that these threats to the future can inspire future studies on wetlands for their hydrological, climatic, ecological, environmental functions and that solutions can be found for humans to interact with nature peacefully and sustainably.

5 Conclusions

Wetlands play a crucial role in Earth systems for their climaticand hydrological-functions. However, reasonably representing the spatial extent and dynamics of small-scale wetlands has been challenging to LSMs and coupled ESMs. This is particularly important and urgent in the PPR as the wetlands are critical to the region's ecology and the hydrological conditions are complex. In this research, we developed a wetland scheme with two modifications to represent wetland dynamics in the Noah-MP LSM. One is modifying the sub-grid saturation fraction to indicate the spatial wetland extent based on grid cell soil moisture. Another is incorporating a dynamic surface water storage scheme to represent the hydrological processes in wetlands. This new wetland scheme is incorporated in single-point, offline regional simulation, and coupled WRF simulation in the PPR.

The single-point simulation showed that the modified sub-grid F_{sat} using the first layer soil saturation reasonably mimics the magnitude and seasonality of surface saturation condition in the PPR, compared to the default TOPMODEL-based formula. The modified increased F_{sat} formula partitions more water to surface runoff than infiltration to soil moisture. The enhanced surface inflow is then collected by the surface storage, mimicking the capacity of wetland depressions, with water exceeding the capacity as fill and spill outflow. The single-point simulation also shows that the wetland modification of surface energy and water balance depends on its maximum capacity. For shallow-storage wetlands, both spring inflow and summer evaporation demand would exceed their maximum capacity, limiting their function in energy and water exchange with the atmosphere.

In the offline regional simulation in the PPR, two spatially varied parameters are incorporated, the maximum F_{satmx} fraction and maximum storage capacity W_{cap}. The results show that the model-simulated wetlands are located in the Northeast portion of the PPR domain, where F_{satmx} is high but maximum capacity is shallow. By incorporating the wetland scheme, the summertime evaporation and latent heat fluxes are evidently increased, with decreasing surface runoff and sensible heat fluxes.

Finally, we examine the wetlands' feedback to regional temperature and precipitation in the coupled WRF-NoahMP-Wetland model. A cooling effect, induced by the presence of wetlands, is evident in all three years' summer for about 0.5~1℃ in a dry year (2006) and 0.7~1.5℃ in a wet year (2005), occurring where the wetland fraction is high. This cooling is the result of wetlands altering energy balance partitioning, increasing latent heat fluxes while reducing sensible heat fluxes. The cooling effect is strongest in July and weakest in May, consistent with the theory of evaporation being energy limited in early summer but transitioning to water limited in mid-summer. In the summer of 2006, when an extreme heatwave hit the Central U.S. and Southern Canada, the presence of wetlands could profoundly reduce the number of extreme hot days by more than 10 during the summer period, effectively reducing the heat stress to human comfort. On the other hand, wetland scheme impacts on regional precipitation do not manifest in an obvious spatial pattern, including both positive and negative effects on precipitation.

Our results show that the presence of wetlands could be beneficial to many sectors by regulating surface runoff during flooding and cooling atmospheric temperatures during heatwaves. These highlights should inspire future studies to understand wetlands' value in regional environments and the Earth system, especially those that have been neglected at the cost of human expansion.

Data Availability Statement

The CONUS WRF simulation over the contiguous US (Liu et al., 2017) can be accessed at https://rda.ucar.edu/datasets/ds612.0/TS1. The simulations data in this study, including the single-point, offline, and coupled WRF simulation for the Prairie Pothole Region can be accessed in a FAIR compliant repository at osf.io:

https://osf.io/nckxy/?view_only=3fa18c1a466a46f1a414ecdaa0c24d67.

The Noah-MP model is driven by the NCAR high-resolution land data assimilation system (Chen et al., 2007) and can be downloaded from https://github.com/NCAR/hrldas/. The Noah-MP LSM can be accessed from https://github.com/NCAR/noahmp.

We appreciate Dr. Catherine Prigent for her help and support in this study and providing the GIEMS data for surface water inundation. The GIEMS data can

be accessed in https://lerma.obspm.fr/spip.php?article91&lang=fr.

References

Badiou, P., McDougal, R., Pennock, D., & Clark, B. (2011). Greenhouse gas emissions and carbon sequestration potential in restored wetlands of the Canadian prairie pothole region. Wetlands Ecology and Management, 19(3), 237–256. https://doi.org/10.1007/s11273-011-9214-6

Badiou, P., Page, B., & Akinremi, W. (2018). Phosphorus Retention in Intact and Drained Prairie Wetland Basins: Implications for Nutrient Export. Journal of Environmental Quality, 47(4), 902–913. https://doi.org/10.2134/jeq2017.08.0336

Barlage, M., Tewari, M., Chen, F., Miguez-Macho, G., Yang, Z. L., & Niu, G. Y. (2015). The effect of groundwater interaction in North American regional climate simulations with WRF/Noah-MP. Climatic Change, 129(3–4), 485–498. https://doi.org/10.1007/s10584-014-1308-8

Barlage, M., Chen, F., Rasmussen, R., Zhang, Z. & Miguez-Macho, G. The importance of scale-dependent groundwater processes in land-atmosphere interactions over the central United States. Geophys. Res. Lett. (2021) doi:10.1029/2020GL092171.

Bechtold, M., De Lannoy, G. J. M., Koster, R. D., Reichle, R. H., Mahanama, S. P., Bleuten, W., Bourgault, M. A., Brümmer, C., Burdun, I., Desai, A. R., Devito, K., Grünwald, T., Grygoruk, M., Humphreys, E. R., Klatt, J., Kurbatova, J., Lohila, A., Munir, T. M., Nilsson, M. B., … Tiemeyer, B. (2019). PEAT-CLSM: A Specific Treatment of Peatland Hydrology in the NASA Catchment Land Surface Model. Journal of Advances in Modeling Earth Systems, 11(7), 2130–2162. https://doi.org/10.1029/2018MS001574

Beven, K. J., & Kirkby, M. J. (1979). A physically based, variable contributing area model of basin hydrology / Un modèle à base physique de zone d'appel variable de l'hydrologie du bassin versant. Hydrological Sciences Bulletin, 24(1), 43–69. https://doi.org/10.1080/02626667909491834

Beven, K. (1997). TOPMODEL: A critique. Hydrological Processes, 11(9), 1069–1085. https://doi.org/10.1002/(SICI)1099-1085(199707)11:9<1069::AID-HYP545>3.0.CO;2-O

Beven, K. J., Kirkby, M. J., Freer, J. E. & Lamb, R. A history of TOPMODEL. Hydrol. Earth Syst. Sci. 25, 527–549 (2021).

Bonan, G. B. (1995). Sensitivity of a GCM Simulation to Inclusion of Inland Water Surfaces. Journal of Climate, 8(11), 2691–2704. https://doi.org/10.1175/1520-0442(1995)008<2691:SOAGST>2.0.CO;2

Bowling, L. C., & Lettenmaier, D. P. (2010). Modeling the effects of lakes and wetlands on the water balance of arctic environments. Journal of Hydrometeorology, 11(2), 276–295. https://doi.org/10.1175/2009JHM1084.1

Dee, D. P., Uppala, S. M., Simmons, A. J., Berrisford, P., Poli, P., Kobayashi, S., Andrae, U., Balmaseda, M. A., Balsamo, G., Bauer, P., Bechtold, P., Beljaars, A. C. M., van de Berg, L., Bidlot, J., Bormann, N., Delsol, C., Dragani, R., Fuentes, M., Geer, A. J., … Vitart, F. (2011). The ERA-Interim reanalysis: configuration and performance of the data assimilation system. Quarterly Journal of the Royal Meteorological Society, 137(656), 553–597. https://doi.org/10.1002/qj.828

Dumanski, S., Pomeroy, J. W., & Westbrook, C. J. (2015). Hydrological regime changes in a Canadian Prairie basin. Hydrological Processes, 29(18), 3893–3904. https://doi.org/10.1002/hyp.10567

Fang, X., & Pomeroy, J. (2020). Diagnosis of future changes in hydrology for a Canadian Rocky Mountain headwater basin. Hydrology and Earth System Sciences Discussions, 1–40. https://doi.org/10.5194/hess-2019-640

Famiglietti, J. S. & Wood, E. F. (1991). Evapotranspiration and Runoff from Large Land Areas: Land Surface Hydrology for Atmospheric General Circulation Models, Surveys in Geophysics, 12, 179-204.

Famiglietti, J. S. & Wood, E. F. Multiscale modeling of spatially variable water and energy balance processes. Water Resour. Res. 30, 3061–3078 (1994a).

Famiglietti, J. S. & Wood, E. F. Application of multiscale water and energy balance models on a tallgrass prairie. Water Resour. Res. 30, 3079–3093 (1994b).

Gardner, Royal C. and Connolly, Kim Diana, The Ramsar Convention on Wetlands: Assessment of International Designations Within the United States (2007). Enviromental Law Review, 37, 1089, Available at SSRN: https://ssrn.com/abstract=983546

Gedney, N., & Cox, P. M. (2003). The Sensitivity of Global Climate Model Simulations to the Representation of Soil Moisture Heterogeneity. Journal of Hydrometeorology, 4(6), 1265–1275. https://doi.org/10.1175/1525-7541(2003)004<1265:TSOGCM>2.0.CO;2

Hatfield, J. L. (2016). Increased Temperatures Have Dramatic Effects on Growth and Grain Yield of Three Maize Hybrids. Agricultural & Environmental Letters, 1(1), 150006. https://doi.org/10.2134/ael2015.10.0006

Hayashi, M., van der Kamp, G., & Rosenberry, D. O. (2016). Hydrology of Prairie Wetlands: Understanding the Integrated Surface-Water and Groundwater Processes. Wetlands, 36, 237–254. https://doi.org/10.1007/s13157-016-0797-9

Hostetler, S. W., Bates, G. T., & Giorgi, F. (1993). Interactive coupling of a lake thermal model with a regional climate model. Journal of Geophysical Research: Atmospheres, 98(D3), 5045–5057. https://doi.org/10.1029/92JD02843

Ireson, A. M., van der Kamp, G., Ferguson, G., Nachshon, U. & Wheater, H. S. Hydrogeological processes in seasonally frozen northern latitudes: understanding, gaps and challenges. Hydrogeol. J. 21, 53–66 (2013).

Ireson, A. M. et al. The changing water cycle: the Boreal Plains ecozone of Western Canada. Wiley Interdiscip. Rev. Water 2, 505–521 (2015).

Koster, R. D., Suarez, M. J., Ducharne, A., Stieglitz, M., & Kumar, P. (2000). A catchment-based approach to modeling land surface processes in a general circulation model: 1. Model structure. Journal of Geophysical Research: Atmospheres, 105(D20), 24809–24822. https://doi.org/10.1029/2000JD900327

Lehner, B., & Döll, P. (2004). Development and validation of a global database of lakes, reservoirs and wetlands. Journal of Hydrology, 296(1–4), 1–22. https://doi.org/10.1016/j.jhydrol.2004.03.028

Liang, X., Lettenmaier, D. P., Wood, E. F., & Burges, S. J. (1994). A simple hydrologically based model of land surface water and energy fluxes for general circulation models. Journal of Geophysical Research, 99(D7), 14415. https://doi.org/10.1029/94JD00483

Liu, C. et al. Continental-scale convection-permitting modeling of the current and future climate of North America. Clim. Dyn. 49, 71–95 (2017).

Melton, J. R., Wania, R., Hodson, E. L., Poulter, B., Ringeval, B., Spahni, R., et al. (2013). Present state of global wetland extent and wetland methane modelling: conclusions from a model inter-comparison project (WETCHIMP). Biogeosciences, 10(2), 753–788. https://doi.org/10.5194/bg-10-753-2013

Miguez-Macho, G., Fan, Y., Weaver, C. P., Walko, R. & Robock, A. Incorporating water table dynamics in climate modeling: 2. Formulation, validation, and soil moisture simulation. J. Geophys. Res. Atmos. 112, 1–16 (2007).

Mishra, V., Cherkauer, K. A., & Bowling, L. C. (2010). Parameterization of lakes and wetlands for energy and water balance studies in the great lakes region. Journal of Hydrometeorology, 11(5), 1057–1082. https://doi.org/10.1175/2010JHM1207.1

Mitra, S., Wassmann, R., Vlek, P. L. G. (2005) An appraisal of global wetland area and its organic carbon stock. Curr Sci 88:25–35

Mitsch WJ, Gosselink JG (2007) Wetlands, 4th edn. Wiley, Hoboken

Valuing wetlands. (2021). Nature Geoscience, 14(3), 111–111. https://doi.org/10.1038/s41561-021-00713-4

Niu, G.-Y., Yang, Z.-L., Dickinson, R. E., & Gulden, L. E. (2005). A simple TOPMODEL-based runoff parameterization (SIMTOP) for use in global climate models. Journal of Geophysical Research, 110(D21), D21106. https://doi.org/10.1029/2005JD006111

Niu, G.-Y., Yang, Z.-L., Mitchell, K. E., Chen, F., Ek, M. B., Barlage, M., et al. (2011). The community Noah land surface model with multiparameterization options (Noah-MP): 1. Model description and evaluation with local-scale measurements. Journal of Geophysical Research, 116(D12), D12109. https://doi.org/10.1029/2010JD015139

Oleson, K. W., Niu, G.-Y., Yang, Z.-L., Lawrence, D. M., Thornton, P. E., Lawrence, P. J., Stöckli, R., Dickinson, R. E., Bonan, G. B., Levis, S., Dai, A., & Qian, T. (2008). Improvements to the Community Land Model and their impact on the hydrological cycle. Journal of Geophysical Research: Biogeosciences, 113(G1), n/a-n/a. https://doi.org/10.1029/2007JG000563

Pattison-Williams, J. K., Pomeroy, J. W., Badiou, P., & Gabor, S. (2018). Wetlands, Flood Control and Ecosystem Services in the Smith Creek Drainage Basin: A Case Study in Saskatchewan, Canada. Ecological Economics, 147, 36–47. https://doi.org/10.1016/j.ecolecon.2017.12.026

Perkins, S. E. (2015). A review on the scientific understanding of heatwaves-Their measurement, driving mechanisms, and changes at the global scale. Atmospheric Research, 164–165, 242–267. https://doi.org/10.1016/j.atmosres.2015.05.014

Pitman, A. (1991). A simple parameterization of sub-grid scale open water for climate models. Climate Dynamics, 6(2), 99–112. https://doi.org/10.1007/BF00209983

Prigent, C., Matthews, E., Aires, F., and Rossow, W. B. (2001). Remote sensing of global wetland dynamics with multiple satellite data sets, Geo. Res. Lett., 28 , 4631-4634

Prigent, C., Papa, F., Aires, F., Rossow, W. B., & Matthews, E. (2007). Global inundation dynamics inferred from multiple satellite observations, 1993–2000. Journal of Geophysical Research, 112(D12), D12107. https://doi.org/10.1029/2006JD007847

Prigent, C., Papa, F., Aires, F., Jimenez, C., Rossow, W. B., & Matthews, E. (2012). Changes in land surface water dynamics since the 1990s and relation to population pressure. Geophysical Research Letters, 39(8), n/a-n/a. https://doi.org/10.1029/2012GL051276

Ringeval, B., Decharme, B., Piao, S. L., Ciais, P., Papa, F., de Noblet-Ducoudré, N., Prigent, C., Friedlingstein, P., Gouttevin, I., Koven, C., & Ducharne, A. (2012). Modelling sub-grid wetland in the ORCHIDEE global land surface model: evaluation against river discharges and remotely sensed data. Geoscientific Model Development, 5(4), 941–962. https://doi.org/10.5194/gmd-5-941-2012

Sivapalan, M., Beven, K., & Wood, E. F. (1987). On hydrologic similarity: 2. A scaled model of storm runoff production. Water Resources Research, 23(12), 2266–2278. https://doi.org/10.1029/WR023i012p02266

Stieglitz, M., D. Rind, J. Famiglietti & C. Rosenzwieg (1997), An Efficient Approach to Modeling the Topographic Control of Surface Hydrology for Regional and Global Climate Modeling, J. Clim., 10, 118-137.

van der Kamp, G., & Hayashi, M. (2009). Groundwater-wetland ecosystem interaction in the semiarid glaciated plains of North America. Hydrogeology

Journal, 17(1), 203–214. https://doi.org/10.1007/s10040-008-0367-1

Wania, R., Melton, J. R., Hodson, E. L., Poulter, B., Ringeval, B., Spahni, R., et al. (2013). Present state of global wetland extent and wetland methane modelling: methodology of a model inter-comparison project (WETCHIMP). Geoscientific Model Development, 6(3), 617–641. https://doi.org/10.5194/gmd-6-617-2013

Zhang, Z., Li, Y., Chen, F., Barlage, M. & Li, Z. Evaluation of convection-permitting WRF CONUS simulation on the relationship between soil moisture and heatwaves. *Clim. Dyn.* (2018) doi:10.1007/s00382-018-4508-5.

Zhang, Z., Li, Y., Barlage, M., Chen, F., Miguez-Macho, G., Ireson, A., & Li, Z. (2020). Modeling groundwater responses to climate change in the Prairie Pothole Region. Hydrology and Earth System Sciences, 24(2), 655–672. https://doi.org/10.5194/hess-24-655-2020
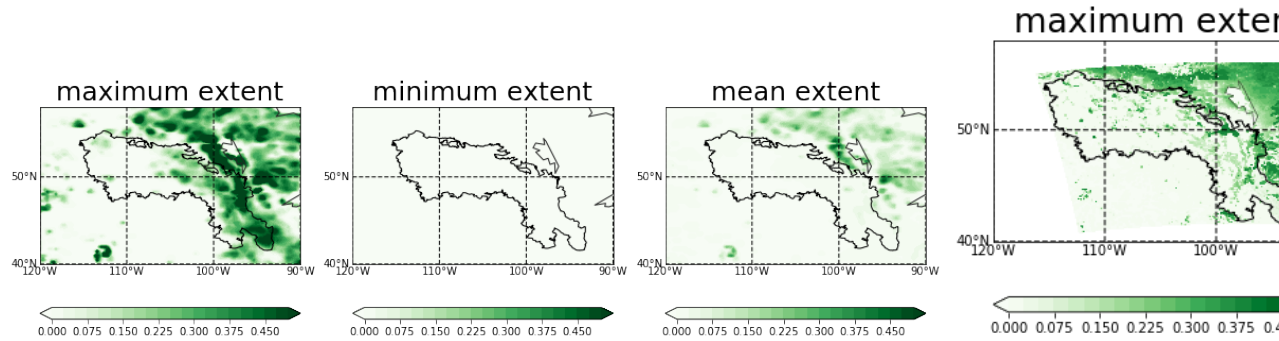
Figures and Tables

Figure 1. Spatial distribution of surface water extent from GIEMS (top) and Noah-MP modeled F_{sat}(bottom), on the maximum, minimum and mean extent.
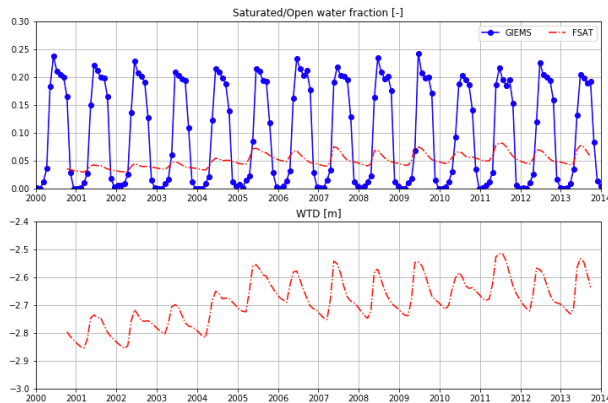
Figure 2. Temporal evolution of the inundation fraction from GIEMS and modelled F_{sat} in the PPR region.
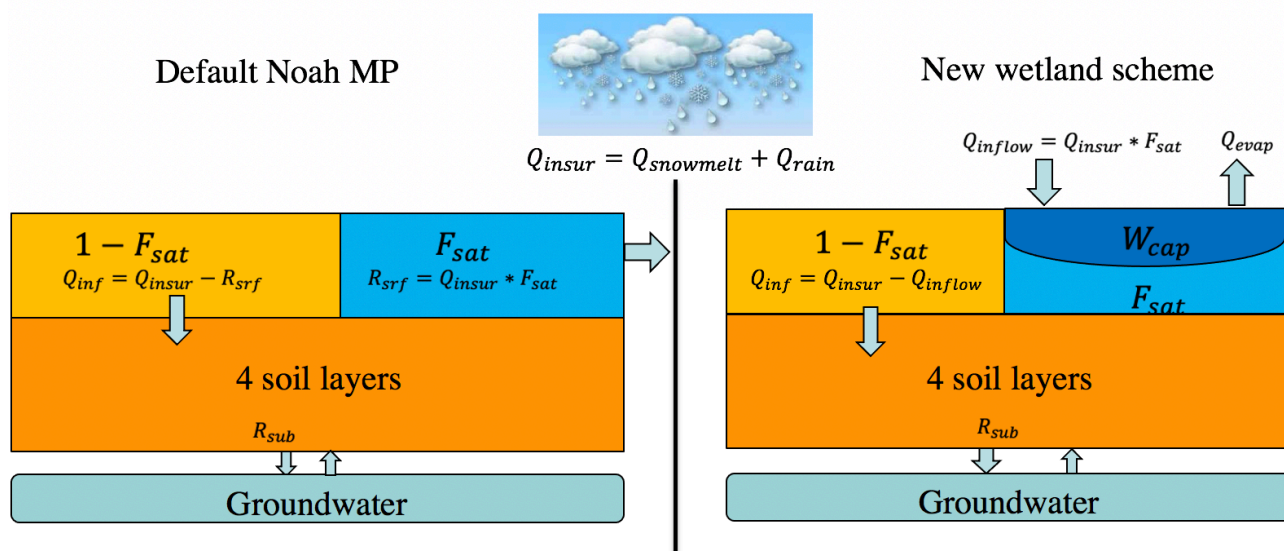
Figure 3. Simple diagram demonstrating the modifications in this study, which includes the modification of surface saturated fraction and the incorporation of a surface wetland storage scheme in Noah-MP LSM.
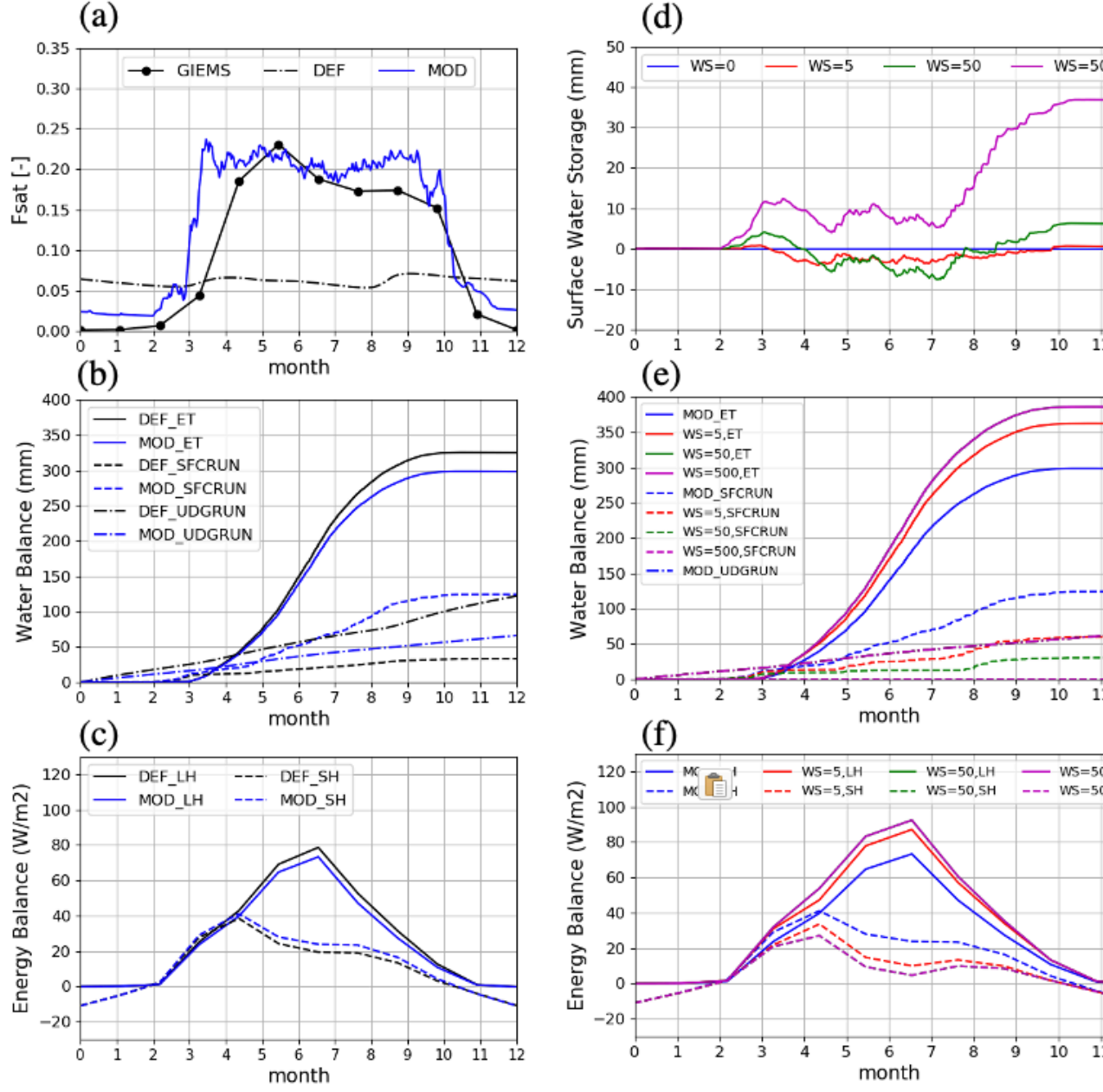
Figure 4. Single-point simulation of F_{sat} modification (a-c) and incorporating dynamic wetland storage (d-f) in Fen site in central Saskatchewan: (a) surface saturated fraction from default and modified formula and GIEMS inundation extent, (b) surface water balance in ET, surface and underground runoff, (c) surface energy balance in sensible and latent heat fluxes; (d) water level change

in wetland storage, (e) surface water balance in ET, surface and underground runoff, (f) surface energy balance in sensible and latent heat fluxes.
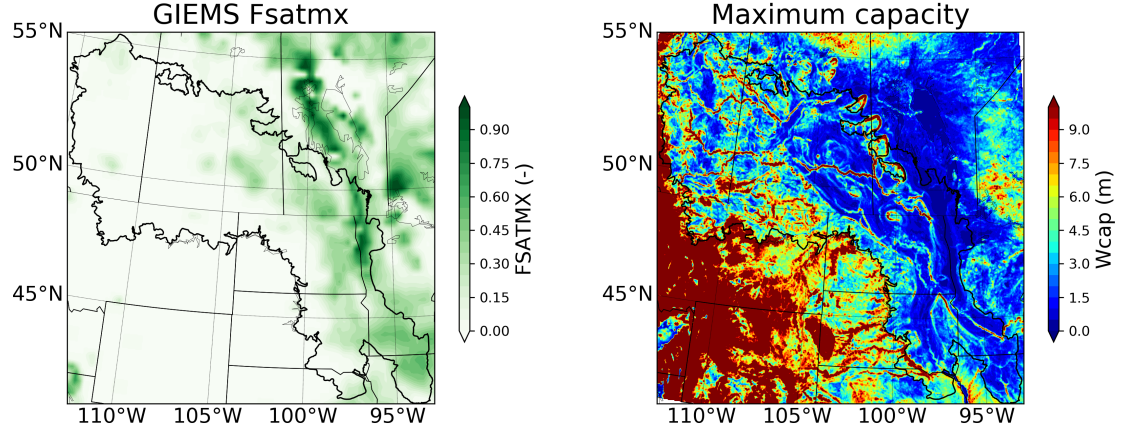
Figure 5. Spatial map of F_{satmx} and W_{cap} in the PPR region, derived from GIEMS product and MERIT DEM, respectively.

Wetland map shows large storage (greater than 200 mm) in North and East of the PPR. In West PPR less than 100 mm (shallow)
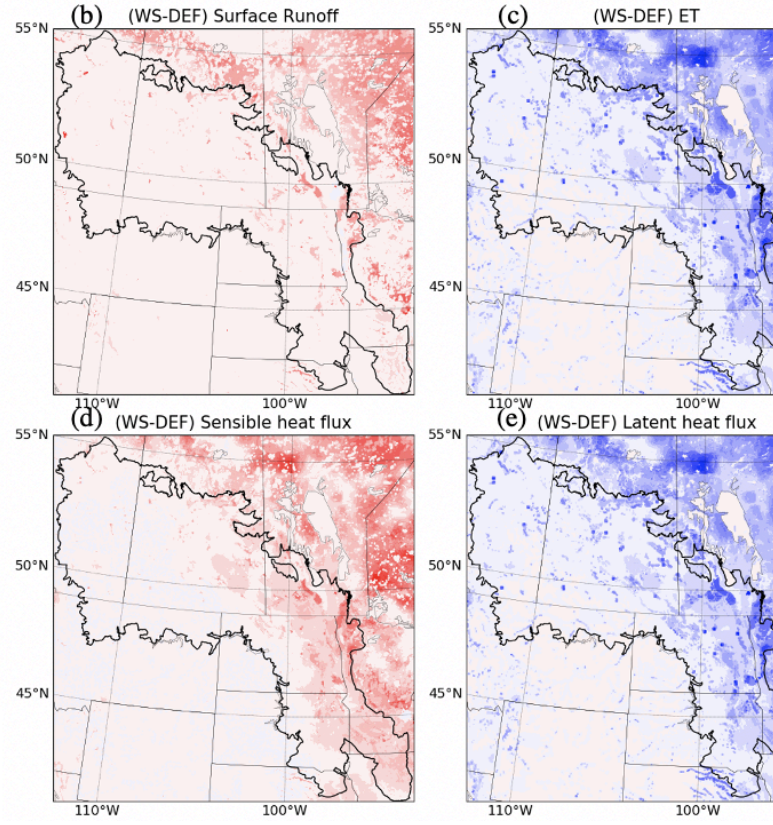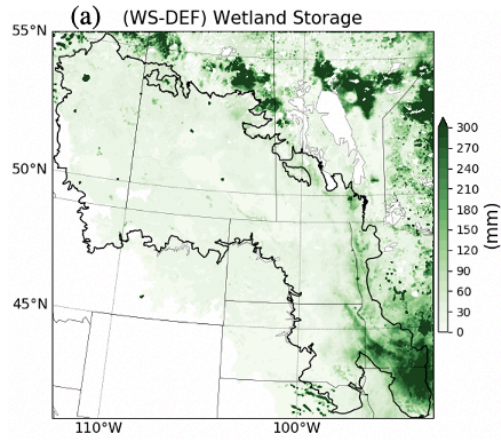

Figure 6. 13-year summertime (MJJA) mean wetland storage level (a); and difference between WS and DEF simulations in surface runoff (b), evapotranspiration (ET, c), sensible heat flux (d), and latent heat flux (e).
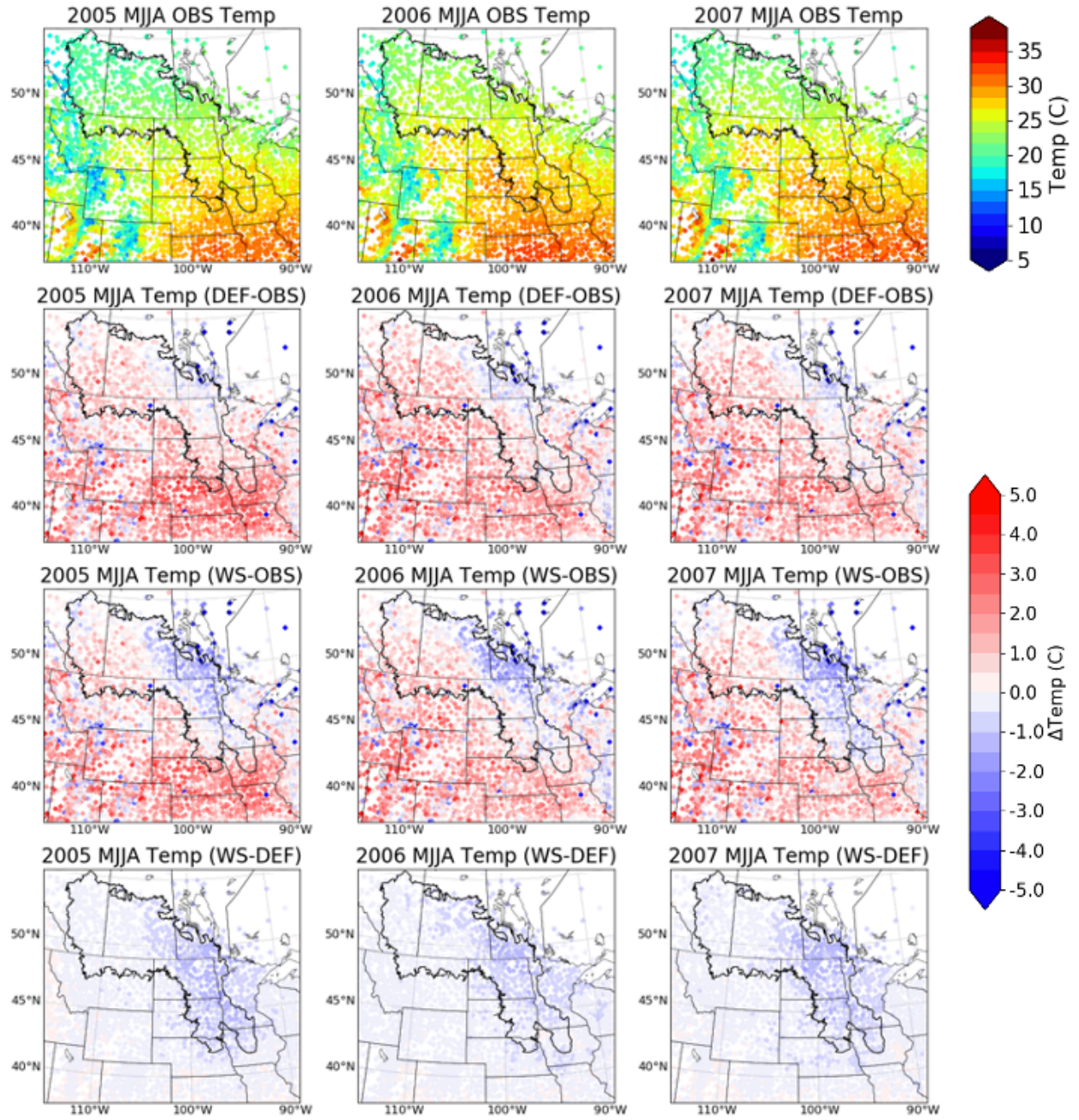
Figure 7. Monthly temperature from station observation, temperature biases from two simulations, and the cooling effect induced by WS in the summer for three-year simulations.
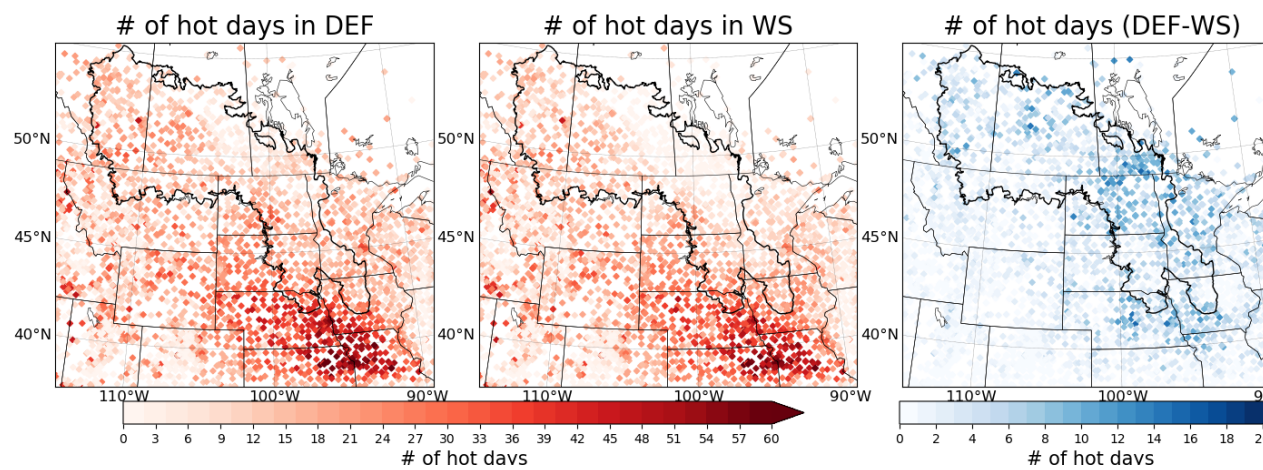
Figure 8. Number of hot days in two simulations and the reduction in hot days from WS to DEF.
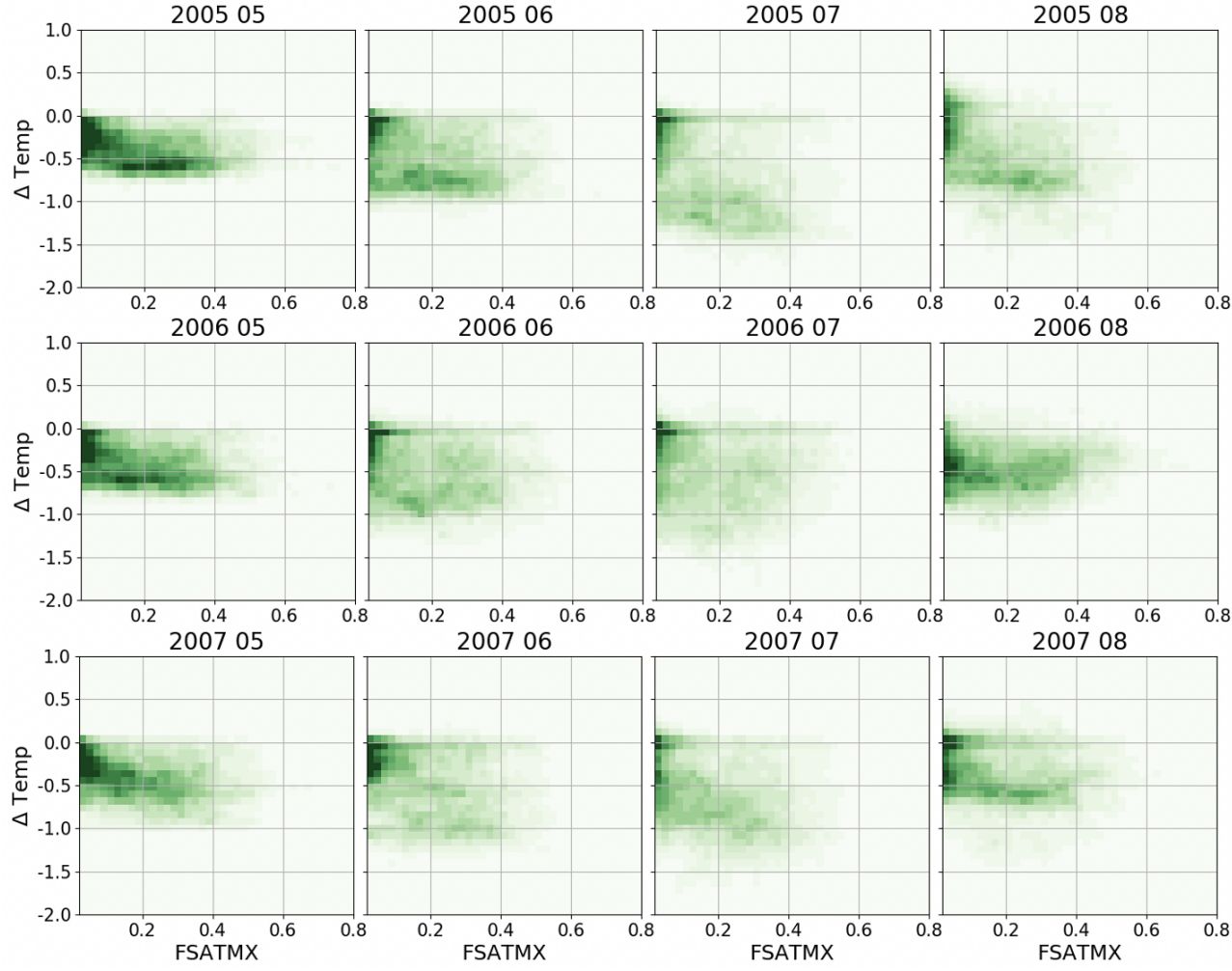
Figure 9. Scatter plot of TEMP (DEF-WS, °C) against the F_{satmx}, maximum saturated fraction in grid cell, from three-year summer monthly data.
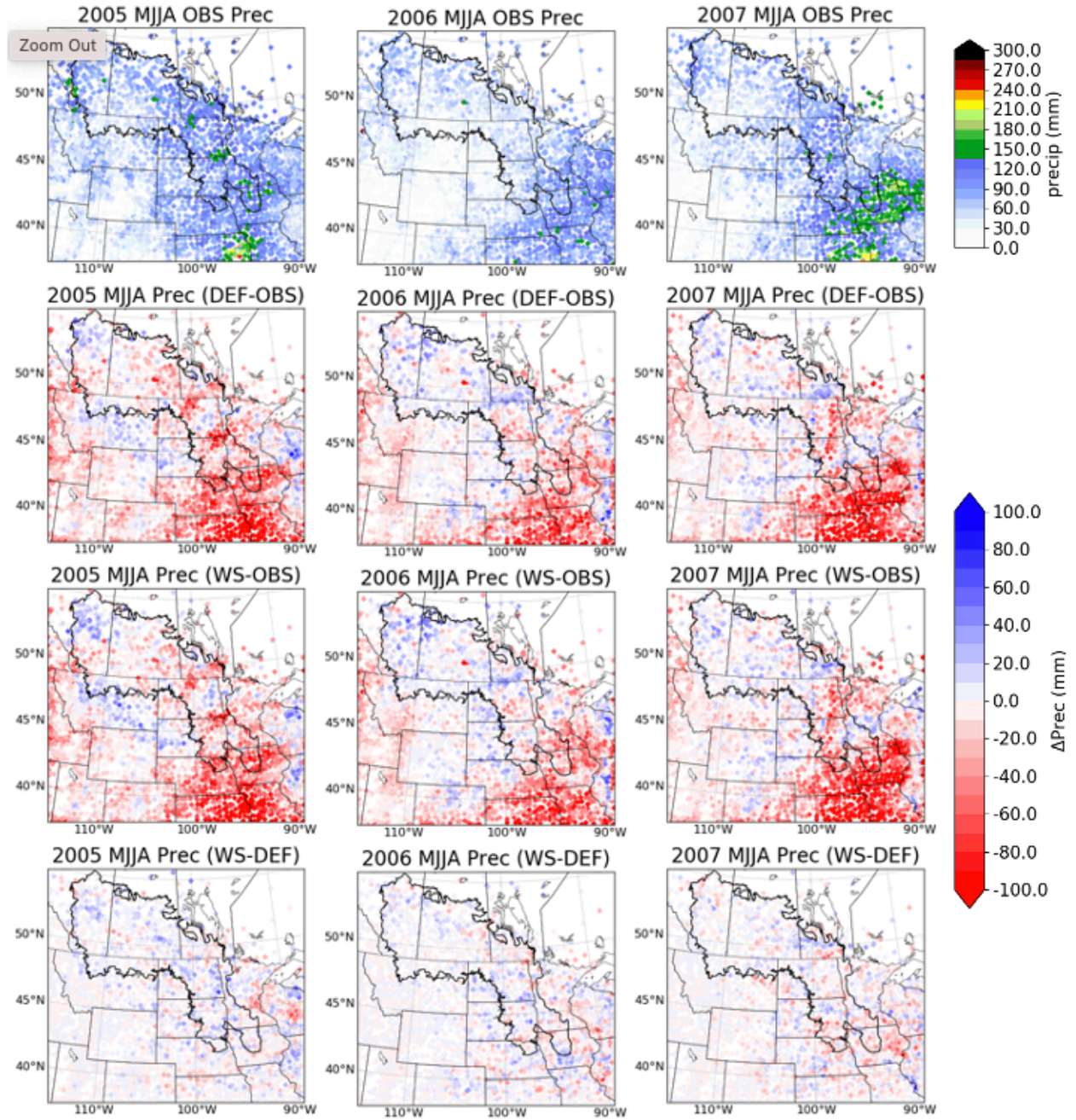
Figure 10. Monthly precipitation from station observation, precipitation biases from two simulations, and the precipitation difference between WS and DEF simulations in the summer for three-year simulations.

Table 1. Summary of the three simulations conducted in this study.

Simulation design	Location	Period	Purpose
Single-point Noah-MP	Fen site, SK	20030101-20101231	Exam the sensitivity
Offline regional Noah-MP	PPR region	20001001-20131001	Incorporate spatially
Coupled regional WRF	PPR region	2005-2007, three summers from Apr to Aug	Conduct coupled W